Identification of potential biomarkers of vascular calcification using bioinformatics analysis and validation *in vivo*

Chuanzhen Chen [1], Yinteng Wu [2], Hai-lin Lu [1], Kai Liu [1], Xiao Qin [Corresp. 1]

[1] Vascular Surgery, Guangxi Medical University First Affiliated Hospital, Nanning, Guangxi Province, China

[2] Orthopedic and Trauma Surgery, Guangxi Medical University First Affiliated Hospital, Nanning, Guangxi Province, China

Corresponding Author: Xiao Qin
Email address: dr_qinxiao@hotmail.com

Background: Vascular calcification (VC) is the most widespread pathological change in diseases of the vascular system. However, we know poorly about the molecular mechanisms and effective therapeutic approaches of VC.

Methods:The VC dataset, GSE146638, was downloaded from the Gene Expression Omnibus (GEO) database. Using the edgeR package to screen Differentially expressed genes (DEGs). Gene set enrichment analysis (GSEA) and gene set variation analysis (GSVA) were used to find pathways affecting VC. Gene ontology (GO) and Kyoto Encyclopedia of Genes and Genomes (KEGG) were performed on the DEGs. Meanwhile, using the String database and Cytoscape software to construct protein-protein interaction (PPI) networks and identify hub genes with the highest module scores. Correlation analysis was performed for hub genes. Receiver operating characteristic (ROC) curves, expression level analysis, GSEA, and subcellular localization were performed for each hub gene. Expression of hub genes in normal and calcified vascular tissues was verified by quantitative reverse transcription PCR (RT-qPCR) and immunohistochemistry (IHC) experiments. The hub gene-related miRNA-mRNA and TF-mRNA networks were constructed and functionally enriched for analysis. Finally, the DGIdb database was utilized to search for alternative drugs targeting VC hub genes.

Results: By comparing the genes with normal vessels, there were 64 DEGs in mildly calcified vessels and 650 DEGs in severely calcified vessels. Spp1, Sost, Col1a1, Fn1, and Ibsp were central in the progression of the entire VC by the MCODE plug-in. These hub genes are primarily enriched in ossification, extracellular matrix, and ECM-receptor interactions. Expression level results showed that Spp1, Sost, Ibsp, and Fn1 were significantly highly expressed in VC, and Col1a1 was incredibly low. RT-qPCR and IHC validation results were consistent with bioinformatic analysis. We found multiple pathways of hub genes acting in VC and identified 16 targeting drugs.

Conclusions: This study perfected the molecular regulatory mechanism of VC. Our results indicated that Spp1, Sost, Col1a1, Fn1, and Ibsp could be potential novel biomarkers for VC and promising therapeutic targets.

1 **Identification of potential biomarkers of vascular calcification using bioinformatics**

2 **analysis and validation in vivo.**

3 Chuanzhen Chen[1], Yinteng Wu[2], Hai-lin Lu[1], Kai Liu[1], Xiao Qin[1]

5 [1]Department of Vascular Surgery, the First Affiliated Hospital of Guangxi Medical

6 University, Nanning 530021, Guangxi Province, China.

7 [2]Department of Orthopedic and Trauma Surgery, the First Affiliated Hospital, Guangxi

8 Medical University, Nanning 530021, China

10 Corresponding Author:

11 Xiao Qin

12 Department of Vascular Surgery, the First Affiliated Hospital of Guangxi Medical

13 University, Nanning 530021, Guangxi Province, China.

14 Email address: dr_qinxiao@hotmail.com.

20 **Abstract**

21 **Background**

22 Vascular calcification (VC) is the most widespread pathological change in diseases of

23 the vascular system. However, we know poorly about the molecular mechanisms and

24 effective therapeutic approaches of VC.

26 **Methods**

27 The VC dataset, GSE146638, was downloaded from the Gene Expression Omnibus

28 (GEO) database. Using the edgeR package to screen Differentially expressed genes

29 (DEGs). Gene set enrichment analysis (GSEA) and gene set variation analysis (GSVA)

30 were used to find pathways affecting VC. Gene ontology (GO) and Kyoto Encyclopedia

31 of Genes and Genomes (KEGG) were performed on the DEGs. Meanwhile, using the

32 String database and Cytoscape software to construct protein-protein interaction (PPI)

33 networks and identify hub genes with the highest module scores. Correlation analysis

34 was performed for hub genes. Receiver operating characteristic (ROC) curves,

35 expression level analysis, GSEA, and subcellular localization were performed for each

36 hub gene. Expression of hub genes in normal and calcified vascular tissues was verified

37 by quantitative reverse transcription PCR (RT-qPCR) and immunohistochemistry (IHC)

38 experiments. The hub gene-related miRNA-mRNA and TF-mRNA networks were

39 constructed and functionally enriched for analysis. Finally, the DGIdb database was

40   utilized to search for alternative drugs targeting VC hub genes.

Results

43   By comparing the genes with normal vessels, there were 64 DEGs in mildly calcified

44   vessels and 650 DEGs in severely calcified vessels. Spp1, Sost, Col1a1, Fn1 and Ibsp

45   were central in the progression of the entire VC by the MCODE plug-in. These hub

46   genes are primarily enriched in ossification, extracellular matrix, and ECM-receptor

47   interactions. Expression level results showed that Spp1, Sost, Ibsp, and Fn1 were

48   significantly highly expressed in VC, and Col1a1 was incredibly low. RT-qPCR and IHC

49   validation results were consistent with bioinformatic analysis. We found multiple

50   pathways of hub genes acting in VC and identified 16 targeting drugs.

Conclusions

53   This study perfected the molecular regulatory mechanism of VC. Our results indicated

54   that Spp1, Sost, Col1a1, Fn1, and Ibsp could be potential novel biomarkers for VC and

55   promising therapeutic targets.

57   **Keywords:** Vascular calcification; Differentially expressed genes; Gene set enrichment

58   analysis; Gene set variation analysis; Protein–protein interaction; Functional enrichment

59   analysis.

Introduction

Vascular calcification (VC) is a pathological process in which calcium phosphate

accumulates in the vessel wall and is the basis for the development and progression of

cardiovascular disease(Strauss et al. 2019). VC occurs mainly in the intima and

intermediate layers of the arterial vasculature(Lee et al. 2020). Intimal calcification is

mainly atherosclerotic plaque caused by chronic inflammation of the vessel, leading to

luminal narrowing and obstruction(Doherty et al. 2003; Durham et al. 2018).

Intermediate calcification is mainly caused by the process of osteogenic differentiation

mediated by vascular smooth muscle cells (VSMCs), leading to the loss of vascular

elasticity(Chen et al. 2020). VC increases with age, with chronic kidney disease, uremia,

hypertension, and diabetes all contributing to this process(Giachelli 2004; Mizobuchi et

al. 2009). Studies have shown that VC is widespread in diabetic patients and that

mortality increases with increasing calcification(Lindholt et al. 2020; Valenti et al. 2016).

We found that calcium and phosphorus metabolism is disturbed in chronic kidney

disease patients, which is a crucial factor contributing to the development of VC(London

et al. 2003; Shroff et al. 2013). VC leads to vascular stiffness and lumen narrowing,

resulting in ventricular hypertrophy and heart failure(Jacob 2003; Scialla et al. 2011). It

has been reported that approximately 40% of deaths in people over 65 years of age are

due to cardiovascular disease(Pescatore et al. 2019). VC is a biomarker for the

development of cardiovascular disease and peripheral vascular disease and is an

80 important factor in the evaluation of health status in the elderly(Budoff et al. 2010).

81

82 In the past, VC has been considered a passive and unavoidable pathological process.

83 However, recent findings suggest that the shift from the VSMCs phenotype to the

84 osteoblast phenotype is a major reason for the occurrence of VC(Leopold 2015). They

85 concluded that VC is an active and regulated process similar to bone development and

86 cartilage formation(Jiang et al. 2021; Towler et al. 2006). These results provide a solid

87 theoretical basis for the study and treatment of VC. Although there have been many

88 studies on the molecular mechanisms underlying the development of VC, effective

89 preventive and therapeutic therapies are still lacking. Therefore, there is an urgent need

90 to further search for hub genes and effective drugs for VC.

91

92 With the completion of the Human Genome Project, high-throughput detection and

93 analysis technologies have been rapidly developed(Bell 2004; Downes et al. 2019;

94 Green et al. 2015). Bioinformatics analysis on the dataset from high-throughput

95 sequencing has become one of the crucial methods in medical science research(Iqbal

96 et al. 2021; Rung & Brazma 2013; Vogelstein et al. 2013; Wheeler & Wang 2013). The

97 development of VC is a diverse and complicated process. We can study the biology of

98 VC from more perspectives through genomics techniques. Analysis of high-throughput

99 sequencing datasets can filter out many DEGs on VC. However, due to the complex

100 molecular regulatory mechanisms of VC molecules, variability among different samples,

101 and the various bioinformatics methods for analysis, some of the DEGs obtained may

102 not be consistent each time. Therefore, to validate the accuracy of DEGs, we can use

103 bioinformatics analysis methods from multiple VC datasets to explore common genes.

104 The Fetuin-A, C5 and OPN protein have been reported to be valid and reliable as a

105 bioinformatic marker of cardiovascular disease(Bostom et al. 2018; Kapetanios et al.

106 2016; Martínez-López et al. 2020; Van Campenhout & Golledge 2009).

107

108 In this study, we used bioinformatics analysis to investigate the molecular regulatory

109 mechanisms of hub genes that influence VC development and explore therapeutic

110 agents that could target hub genes. We obtained DEGs between calcified and normal

111 vessels from GSE146638, a gene expression profile downloaded from the GEO

112 database. In addition, this dataset was performed with GSEA and GSVA to search for

113 the biological pathways in VC. Immediately after, we performed GO and KEGG analysis

114 on these DEGs. By constructing PPI networks, we screened for the highest scoring

115 modules and hub genes. To validate that these hub genes can serve as markers of VC,

116 we calculated each hub gene's ROC curve area and expression levels in the uremia-

117 induced VC and the normal groups. VC models were constructed to verify the

118 expression levels of hub genes using RT-qPCR and immunohistochemistry. The

119 pathways through which hub genes affect VC were explored using GSEA.

120 We then searched for miRNAs targeting regulated hub genes using the miRDB,

121 miRWALK, and Targetscan databases and for target-regulated transcription factors

122 using the KnockTF database. We constructed miRNA-mRNA and TF-mRNA networks

123 and performed functional enrichment analysis on them. We identified 16 drugs that

124 regulate hub genes affecting VC using the DGIdb database. This study will improve our

125 understanding of the molecular mechanisms of VC and provide genomic-targeted

126 therapy options for VC. And the process of our study is shown in Figure 1.

127

128 ***Material and Methods***

129 **Data acquisition and differential expression analysis**

130 The RNA expression profile GSE146638 was obtained from the GEO database

131 (https://www.ncbi.nlm.nih.gov/geo). It includes 5 normal samples, 5 samples with VC

132 caused by uremia, and 4 samples with VC caused by vitamin D3. According to Jakob's

133 study, severe VC occurred in rats with uremia and slight VC in rats with vitamin

134 D3(Rukov et al. 2016). We respectively compared these two groups of samples with

135 different degrees of VC with control samples. After obtaining the gene expression

136 matrix, we used the edgeR package to look for DEGs between calcified and normal

137 vessels using |log2FC|>1 and FDR<0.05 as cutoff criteria. To improve obtaining

138 accurate and reliable DEGs, we used the VennDetail website to separate the

139 intersection of the two groups' upregulated and downregulated DEGs.

140

141 **GSEA and GSVA**

142 To find GO and KEGG entries affecting VC, we performed GSEA on normal and

143 uremia-induced VC samples using the "clusterprofiler" R package, defining that

144 pathways matching |NES|>1, p-val<0.05 and q-val<0.05 were significantly enriched.

145 Also, using "c2.cp.kegg.v7.4.entrez.gmt" and "c5.all.v7.4.entrez.gmt" as background

146 gene sets, we performed a GSVA on normal and uremia-induced VC samples using the

147 "GSVA" R package to explore further GO and KEGG entries affecting VC.

148

149 **Functional enrichment analysis of DEGs**

150 To better investigate the biological functions of DEGs, we performed functional

151 enrichment analysis of vascular calcified DEGs using the "clusterprofiler" R package,

152 which includes GO and KEGG pathways analysis, with *P*<0.05 being statistically

153 significant. GO analysis includes biological processes (BP), cellular components (CC),

154 and molecular functions (MF).

155

156 **PPI Network and correlation analysis among hub genes**

157 We constructed PPI networks using STRING (http://string-db.org) database and

158 Cytoscape software for both sets of DEGs, and the significance threshold was set to an

159 interaction score >0.4. The highest scoring modules were screened using the MCODE

160 plugin of Cytoscape software, and the genes in the modules were defined as hub

161 genes. We performed functional enrichment analysis of the hub genes in the highest-

162 scoring modules using the Metascape (http://metascape.org) database. In addition, we

163 obtained information of hub genes in VC and normal groups and explored the

164 correlation between hub genes using the "corrplot" R package. GO annotation data

165 were constructed from BP, CC, and MF levels using the "GOSemSim" R package to

166 examine further whether hub genes are directly functionally similar. The geometric

167 mean of these genes at the BP, CC, and MF levels was calculated to obtain a final

168 score for a comprehensive assessment of the gene's function in the three groups.

169

170 **ROC curves and expression of hub genes**

171 To evaluate the ability of these hub genes to distinguish calcified vessels from normal

172 vessels, we extracted the expression profiles of hub genes in normal samples and

173 uremia-induced VC samples. We plotted ROC curves for each hub gene using the

174 "proc" R package. Meanwhile, we extracted the expression profiles of hub genes in

175 normal samples and uremia-induced VC samples and visualized each hub gene's

176 expression level using the "ggplot2" R package.

177

178 **Construction of miRNA-mRNA and TF-mRNA networks and Functional enrichment**

179 **analysis**

180 Both miRNAs and transcription factors (TFs) can play a role in maintaining physiological

181 stability by regulating the expression of target genes. We used miRWALK

182 (http://mirwalk.umm.uni-heidelberg.de), miRDB (http://www.mirdb.org) and Targetscan

183 (http://www.targetscan.org) databases to find miRNAs regulating Hub genes, taking the

184 intersection of the results of these three databases. We used the KnockTF

185 (http://www.licpathway.net/KnockTF/index.html) database to find transcription factors

186 that regulate Hub genes. In addition, we visualized miRNA-mRNA and TF-mRNA

187 networks with Cytoscape software and performed functional enrichment analysis of

188 miRNA-mRNA networks and TFs-mRNA networks using the Metascape database.

189

190 **Drug-Gene Interactions**

191 We used the DGIdb (https://www.dgidb.org) database to retrieve the drugs targeting the

192 hub genes of VC. Types of drug action include activation, inhibition and unknown.

193

194 **GSEA and Subcellular localization of each hub gene**

195 To explore the function of each hub gene in VC, we divided each hub gene into high

196 and low expression groups using the median expression level of each hub gene as the

197 cut-off point. We performed GSEA on each hub gene using the "clusterprofiler" R

198 package, setting the pathways meeting the criteria of |NES|>1, p-val<0.05, and q-

199 val<0.05 as significantly enriched. The localization of mRNA is an evolutionarily

200 conserved phenomenon that controls many important biological processes, and the

201 function of mRNA is closely related to its localization in the cell. To further understand

202 the mechanism of hub genes involved in calcification, we obtained FASTA files of Spp1,

203 Sost, Ibsp, Col1a1, and Fn1 from the Gene database and subsequently used the

204 mRNALocater database to predict the subcellular localization of these genes.

205

206 **Ethical Statements and Establishment of a rat model of VC**

207 All the animal experiments were approved by the Ethics Committee of Guangxi Medical

208 University (Approval Number: 201910030). Our studies conformed to the guidelines for

209 the care and use of laboratory animals published by the Chinese Academy of Health

210 Sciences. We obtained male Sprague Dawley rats weighing approximately 180 g from

211 the Experimental Animal Center of Guangxi Medical University for the study. These rats

212 were housed in a specific antigen-free environment and provided with adequate food

213 and water.

214

215 We randomly divided the animals into two groups of 10 animals each. The VC model

216   was established by intraperitoneal injection of vitamin D3 300,000 IU/kg once daily for

217   14 days. To ensure the univariate principle of the experiment, the negative control group

218   was injected with an equal amount of saline. The rats were treated with the cervical

219   dislocation method at the end of the experiment, and then the aorta was collected.

220

RT-qPCR experiments of aorta

222   To measure the expression of Spp1, Sost, Ibsp, Col1a1, and Fn1 in calcified vessels,

223   we performed reverse transcription and real-time fluorescence polymerase chain

224   reaction on RNA. The primers used are shown in Table 1. Spp1, Sost, Ibsp, Col1a1 and

225   Fn1 expressions were normalized by β-actin, with the relative expressions calculated by

226   comparison with the $2^{-\Delta\Delta CT}$ method.

227

Alizarin red staining, Von kossa staining and immunohistochemical experiments

of aorta

230   We fixed the thoracic aorta in 4% paraformaldehyde and embedded it in a wax block.

231   We cut the wax block into 5 um sections, and the sections were dewaxed with xylene

232   and dehydrated with the alcohol solution. For Alizarin red staining, we placed the

233   sections in Alizarin red staining solution for 5 minutes and then photographed them

234   under a light microscope. For Von Kossa staining, we incubated the sections in 1%

235 silver nitrate in sunlight for 1 hour followed by 2% sodium thiosulfate for 2 minutes, and

236 then photographed with a light microscope. Positively stained areas were detected

237 using ImageJ analysis. For immunohistochemical staining of thoracic aorta, we removed

238 paraffin from the sections, dehydrated them in graded alcohol solution, closed them with

239 5% fetal bovine serum for 1 hour, and stained them with Spp1 (22952-1-AP 1:100), Sost

240 (21933-1-AP 1:100), Ibsp (ABP60403 1:200), Col1a1 (67288-1-Ig 1:2500) and Fn1

241 (66042-1-Ig 1:500) primary antibodies were soaked overnight at 4°C. The following day,

242 we incubated the sections with the corresponding secondary antibodies for 1 hour at

243 room temperature. According to the manufacturer's requirements, we first stained with

244 the DAB kit, repeated the staining with hematoxylin, and then photographed with a light

245 microscope. ImageJ was used to analyze the positively stained areas.

246

247 **Statistical Analysis**

248 The data set was analyzed using Rstudio (version 4.0.2). Differential expression

249 analysis was performed using t-test to determine p-values and FDR. All results are

250 expressed as mean ± SD. We performed statistical analysis of the results by Student's

251 t-test using GraphPad Prism software. $P<0.05$ was considered statistically significant.

252

Results

Identification of DEGs in VC

Comparing the genes of uremia-induced VC with normal samples in GSE146638, we

found 650 DEGs, including 405 up-regulated and 245 down-regulated genes (Fig 2A).

Comparing the genes of vitamin D3-induced VC with those of normal vessels in

GSE146638, we found 64 DEGS, including 42 up-regulated and 22 down-regulated

genes (Fig 2B). We then intersected the results of the two groups of up-and down-

regulated DEGs separately to obtain a set of DEGs containing 5 down-regulated genes

(Fig 2C) and 9 up-regulated genes (Fig 2D).

The result of GSEA and GSVA

GO and KEGG analysis of genes between uremia-induced VC and normal groups were

performed by using the GSEA method. In GO BP analysis, genes were primarily rich in

antigen processing and peptide antigen presentation, positive regulation of leukocyte

cell adhesion and cell activation (Fig 3A). In GO CC analysis, genes were mainly rich in

MHC protein complexes, mitochondrial respiratory chain complex I (Fig 3B). In GO MF

analysis, genes were mainly rich in glycosaminoglycan binding, heparin-binding and

receptor-ligand activity (Fig 3C). In KEGG pathway analysis, genes were rich in allograft

rejection, reactive oxygen species separation, and ECM-receptor (Fig 3D). Also, we

272   performed GSVA on genes from uremia-induced VC and normal samples. In GO

273   analysis, genes from VC samples were mainly rich in cytoskeleton organization,

274   phosphoprotein binding, and Transporter vesicles (Fig 4A). In KEGG analysis, genes

275   were rich in Koinuma targets of smad2 or smad3 and Gobert oligodendrocyte

276   differentiation (Fig 4B).

277

278   **Functional enrichment analysis and pathway of DEGs**

279   We performed GO and KEGG pathway analysis of DEGs in the uremia-induced VC

280   group and normal controls. In GO BP analysis, we found that DEGs were rich in

281   ossification and response to glucocorticoid (Fig 5A). In GO CC analysis, DEGs were

282   rich in lysosomes, cell vacuoles, and extracellular matrix (Fig 5B). In GO MF analysis,

283   DEGs were mainly rich in amide binding, cell adhesion molecule binding, and sulfur

284   compound binding (Fig 5C). In KEGG pathway analysis, DEGs were primarily rich in

285   human T-cell leukemia virus 1 infection, focal adhesion and lysosomes (Fig 5D).

286

287   **PPI network construction, hub genes identification and correlation between hub**

288   **genes**

289   We constructed and analyzed PPI networks for two groups of DEGs with different

290   degrees of VC using the STRING database and Cytoscape software. In the uremia-

291   induced VC group, 571 DEGs with a score >0.4 were selected for PPI network

292   construction (Fig 6A). In the vitamin D3-induced VC group, 36 DEGs with scores >0.4

293   were selected for PPI network construction (Fig 6B). We also constructed a PPI network

294   for the intersection of DEGs with two different degrees of VC. And the most significant

295   module consisting of 5 genes and 18 edges was found using the MCODE plug-in of

296   Cytoscape software (Fig 6C). Next, we performed functional enrichment analysis of

297   these hub genes using the Metascape database (Fig 6D). In GO BP analysis, we found

298   that hub genes were rich in ossification, response to steroid hormones, and response to

299   mechanical stimulation. In GO CC analysis, hub genes were rich in the extracellular

300   matrix. In GO MF analysis, hub genes were rich in cell adhesion molecule binding, and

301   integrin binding. And in KEGG pathway analysis, hub genes were rich in ECM-receptor

302   interaction. In addition, correlation analysis of hub genes (Spp1, Sost, Col1a1, Fn1, Ibsp

303   ) was highly correlated (Fig 6E). Also, these five hub genes were functionally related,

304   with IBSP occupying the most significant position (Fig 6F).

305

306   **ROC curves and expression of hub genes**

307   We constructed ROC curves of each hub gene separately and found that their area

308   under ROC curves of Sost, Ibsp, Fn1, Col1a1, and Spp1 were all close to 1 in the

309   uremia-induced VC group in GSE146638, with the normal group as control (Fig 7A).

310   These indicate that these five genes have a good ability to discriminate between

311   calcified and normal vessels. Meanwhile, by verifying the expression of these hub

312   genes in the uremia-induced VC group (Fig 7B), we found that Sost, Ibsp, Fn1, and

313   Spp1 were highly expressed in calcified samples, while Col1a1 was lowly expressed.

314

Validation of hub gene expression in rat aorta with VC

316   By performing Alizarin red staining and Von kossa staining on the aorta, we found

317   significant calcium salt deposition on the aortic wall of rats induced with vitamin D3,

318   which indicated that the constructed model of vascular calcification was successful(Fig

319   8A). We demonstrated by RT-qPCR experiments that Sost, Ibsp, Fn1, and Spp1 mRNA

320   expression were highly expressed in the calcified aorta, while Col1a1 mRNA was lowly

321   expressed (Fig 8B). Also, we demonstrated by immunohistochemistry experiments that

322   Sost, Ibsp, Fn1, and Spp1 protein expression were highly expressed in the calcified

323   aorta, while Col1a1 protein was lowly expressed (Fig 8C).

324

GSEA and Subcellular localization of hub genes

326   By performing GSEA analysis of each hub gene, we found that Ibsp, Sost, Fn1, and

327   Spp1 were primarily rich in allograft rejection, ECM -receptor interaction and

328   phagosome. And Col1a1 were primarily rich in citrate cycle and oxidative

329   phosphorylation (Fig 9A-E). We found that Sost and Col1a1 were mainly distributed in

330   the cytoplasm, and Ibsp, Spp1 and Fn1 were primarily distributed in the nucleus (Fig

331   9F). They play similar roles although they are mainly distributed in different locations of

332   the cell.

333

334   **Construction and Functional enrichment analysis of miRNA-mRNA networks and**

335   **TF-mRNA networks**

336   We searched for target-regulated hub gene miRNAs using miRWALK, miRDB, and

337   Targetscan databases and then used the results of these databases as intersections.

338   By constructing miRNA-mRNA networks, we found 109 miRNAs targeting regulation of

339   Col1a1, 94 miRNAs targeting regulation of Fn1, 25 miRNAs targeting regulation of Ibsp,

340   49 miRNAs targeting regulation of Sost, and Spp1 regulated by 18 miRNAs (Fig 10A).

341   Meanwhile, we found that miRNA-mRNA network functional enrichment analysis

342   primarily focused on gene silencing, ossification, and ECM-receptor interactions of

343   miRNAs (Fig 10B). We used the KnockTF database to search for target-regulated hub

344   gene transcription factors. We found 80 TFs regulating Col1a1, 45 TFs regulating Fn1,

345   48 TFs regulating Ibsp, 38 TFs regulating Sost, and 37 TFs regulating Spp1 (Fig 11A).

346   Meanwhile, we found that TF-mRNA network functional enrichment analysis mainly

347   focused on mRNA metabolic processes, myeloid cell differentiation, stem cell

348   differentiation, and transcriptional regulator complexes (Fig 11B).

349

350 **Drug‑gene interaction**

351 We identified 16 drugs that target these hub genes using the DGIdb database (Fig 12).

352 We found that Blosozumab, Romosozumab, and Setrusumab act on Sost, Daidzein and

353 Insulin act on Ibsp, and L19il2, L19sip131l, L19tnfa, and Ocriplasmin act on Fn1,

354 Ocriplasmin and Collagenase clostridium histolyticum act on Col1a1, Tacrolimus,

355 Calcitonin, Alteplase, Gentamicin, Ask-8007, and Wortmannin all act on Spp1. These

356 offer the possibility of genetic treatment of VC.

357

358 *Discussion*

359 VC is a normal part of aging, but diabetic nephropathy and chronic kidney disease,

360 among others, can exacerbate this pathological process. Failure of early screening and

361 diagnosis of VC leads to progressive worsening of the lesion. The degree of VC

362 seriously affects the recovery from cardiovascular system diseases and is one of the

363 vital indicators to evaluate the health status of the elderly. Therefore, the study of

364 biomarkers of VC is significant for the early diagnosis and treatment of the disease.

365 With the development of high-throughput sequencing technology, it has started to be

366 widely applied to find the hub genes of diseases. The re-analysis of sequencing data

367 provides a convenient and comprehensive platform to reveal the molecular mechanism

368 of VC occurrence and find effective target drugs for the treatment of VC.

369

370   In this study, we analyzed the VC expression profile GSE146638 screened from the

371   GEO database. It includes 5 normal samples, 5 samples with severe VC caused by

372   uremia, and 4 samples with mild VC caused by vitamin D3. Compared to normal

373   controls, we found 64 DEGs (including 42 up-regulated and 22 down-regulated) in the

374   vitamin D3-induced VC group and 650 DEGs (including 405 up-regulated and 245

375   down-regulated) in the uremia-induced VC group. We performed GO and KEGG

376   analysis on DEGs. In GO analysis, we found that DEGs were rich in ossification,

377   lysosomes, and extracellular matrix. In KEGG pathway analysis, DEGs were primarily

378   rich in Staphylococcus aureus infection、FoxO signaling pathway、Human T-cell

379   leukemia virus 1 infection、Focal adhesion and Lysosomes. Some of these pathways

380   are involved in the process of VC. Intrinsic stiffness and extracellular matrix remodeling

381   of VSMC contribute to osteogenic differentiation and calcification of VSMC, and

382   ossification and calcification are closely related(Chen et al. 2020). Disruption of

383   extracellular matrix integrity can attenuate medial aortic calcification in its early

384   stages(Uto et al. 2021). Upregulation of FOXO1/3 inhibits VC(Deng et al. 2015). Mitral

385   annular calcification (MAC) may act as a nidus for infection, especially with

386   Staphylococcus aureus infection(Pressman et al. 2017).

387

388   We constructed a PPI network for these DEGs and screened for a top-scoring gene

389   module (Spp1, Sost, Col1a1, Fn1, Ibsp). Meanwhile, we found that these module genes

390   were involved in the whole process of VC progression. We performed the functional

391 enrichment analysis of these hub genes. In GO BP analysis, hub genes were mainly

392 rich in ossification, response to mechanical stimulation, and vascular development. In

393 GO CC analysis, hub genes were rich in the extracellular matrix. In GO MF analysis,

394 hub genes were rich in cell adhesion molecule binding, and integrin binding. And in

395 KEGG pathway analysis, hub genes were enriched in ECM receptor interaction.

396 Numerous studies have shown that VC is mainly produced by the process of osteogenic

397 differentiation mediated by VSMCs(Massy et al. 2008; Shroff et al. 2008).

398 Hypothyroidism and vitamin D deficiency are associated with various cardiovascular

399 diseases, including hypertension, atherosclerosis, VC, and renal failure(Khundmiri et al.

400 2016; Pilz et al. 2016). Matrix GLA proteins have a huge role in maintaining arterial

401 vascular stability, and the lack of matrix GLA promotes VC(El-Maadawy et al. 2003; Luo

402 et al. 1997). These results indicate that our approach to studying VC by bioinformatics is

403 accurate and effective. We found that these hub genes have a strong ability to

404 distinguish whether they are VC or not. In the **VC expression profile GSE146638**, we

405 found that the expression of Ibsp, Sost, Fn1 and Spp1 was high in samples with VC,

406 while the expression of Col1a1 was low in samples with VC. In addition, our results from

407 RT-qPCR and immunohistochemistry experiments were consistent with those in the

408 dataset. Previous studies have shown that high expression of Fn1 is found in arterially

409 calcified aorta and may induce VC through the ERK pathway(Ding et al. 2006). Spp1

410 may prevent high phosphorus-induced renal calcification and VC(Paloian et al. 2016).

411 Sost prevents VC through a negative feedback mechanism(Catalano et al. 2020; De

412 Maré et al. 2019). We found that Ibsp is highly expressed in human calcified

413 plaques(Ayari & Bricca 2012). Col1a1 has been less studied in VC, and the exact

414 molecular regulatory mechanism remains unclear. It has been shown that activation of

415 parathyroid hormone receptors inhibits Col1a1 expression and attenuates aortic

416 fibrosis(Cheng et al. 2010).

417

418 To further search for mechanisms of action that affect VC, we used GSVA and GSEA to

419 search for pathways associated with VC. The use of GSEA identified several pathways

420 that affect VC, such as ECM-receptor interaction and Hematopoietic cell lineage.

421 Alterations in the extracellular matrix are associated with atherosclerosis, restenosis,

422 and heart failure(Chistiakov et al. 2013). Extracellular matrix (ECM) proteins are the first

423 component contributing to atherosclerosis(Lacolley et al. 2017). Post-translational

424 modification of PAR initiates biomineralization by concentrating calcium into spherical

425 structures that can form apatite minerals on the ECM(Duer et al. 2020). Platelets

426 represent the cellular interface between hemostasis, inflammation, and atherosclerosis

427 and have myeloid precursors that promote atherosclerosis(Foresta et al. 2013). Also, by

428 GSVA analysis, we identified multiple pathways affecting VC such as cytoskeleton

429 organization, and apoptotic process. Small contractions of the cytoskeleton may attach

430 integrins to sites on matrix proteins. This results in a sensation of stiffness, which may

431 be caused by the release of differentiation factors through the deformation of binding

432 proteins (Hsu et al. 2016). Apoptosis is a factor that promotes vascular calcification in

433 patients with chronic kidney disease (CKD), and MitoQ inhibits vascular calcification by

434 suppressing apoptosis of vascular smooth muscle cells (VSMC) via the Keap1/Nrf2

435 pathway (Cui et al. 2020).

436

437 The complexity and diversity of VC have hindered our accurate understanding of the

438 disease and the discovery of drugs with precise targets. In this study, we used a

439 comprehensive bioinformatics approach to find hub genes that influence the

440 progression of VC and the drugs that target hub genes. Although some of hub genes

441 have been studied, the molecular mechanisms behind VC remain unclear. Therefore,

442 we predicted miRNAs and transcription factors that regulate central genes and

443 constructed miRNA-mRNA and TF-mRNA networks, respectively. Some of these

444 miRNAs and transcription factors have been shown to play an integral role in the

445 pathology of vascular calcification. miR-29b-3p attenuates vascular calcification by

446 regulating matrix metalloproteinase 2 (Jiang et al. 2017). miR-25 protects

447 glucocorticoid-induced apoptotic process in VSMCs thereby reducing vascular

448 calcification (Zhang et al. 2019). miR-134-5p exacerbates vascular calcification by

449 regulating the expression of histone deacetylase 5 in high phosphate conditions (Choe

450 et al. 2020b). CircSmoc1-2 attenuates vascular calcification by regulating the miR-874-

451 3p/Adam19 axis (Ryu et al. 2022). miR-26-5p affects the pathological process of VC in

452 patients with chronic kidney disease by regulating PTEN expression (Chang et al.

453 2020). miR-27a-3p attenuates vascular calcification by regulating activating transcription

454 factor 3 (an osteogenic transcription factor) (Choe et al. 2020a). Krupp-like factors 4 is a

455 zinc-finger transcription factor and synergizes with RUNX2 to enhance arterial

456 calcification (Yoshida et al. 2012). SOX transcription factor affects endothelial-

457 mesenchymal transition leading to vascular calcification (Yao et al. 2019). Deacetylation

458 of Sp1 reduced the binding of Sp1 to the BMP2 promoter, thereby reducing apoptosis

459 and calcium deposition (Zhang et al. 2021). The transcription factor XBP1,

460 synergistically with runx2, is involved in VC due to oxidative stress (Liberman et al.

461 2011). TEAD4 is a nuclear transcription factor that inhibits vascular calcification by

462 regulating the Wnt/β-Catenin signaling pathway (Cong et al. 2021). By intervening in VC

463 hub genes, it may be a new direction for individualized genomic therapy of VC.

464

465 Vascular calcification can be caused by various diseases, but there is no effective

466 treatment to reduce or reverse vascular calcification. Current therapy of VC is primarily

467 through correction of mineral metabolism markers such as calcium, vitamin D,

468 parathyroid hormone (PTH), and phosphorus (Singh et al. 2021). Clinical investigations

469 of drugs used to treat VC include phosphate binders, calcium mimetics,

470 bisphosphonates, vitamin D, and vitamin K. Bisphosphonates inhibit nucleation and

471 growth of hydroxyapatite and have been used to treat osteoporosis(Lomashvili et al.

472 2009). In uremic animals, pamidronate and etidronate inhibit vascular calcification

473 independent of bone resorption(Giger et al. 2013). Vitamin K promotes blood clotting

474 and calcification homeostasis(Shea & Booth 2019). Sodium thiosulfate chelates calcium

475   to form highly soluble complexes, thereby inhibiting VC(Schlieper et al. 2009). IP6

476   hinders VC by inhibiting hydroxyapatite microcrystals II without directly affecting calcium

477   and phosphorus blood levels(Ferrer et al. 2018). TNAP is a tissue non-specific alkaline

478   phosphatase (ALP) isoenzyme that provides a site for bone mineralization by

479   inactivating pyrophosphate and upregulating phosphate ion levels. Inhibitors targeting

480   TNAP are under investigation(Singh et al. 2021).

481

482   Current treatments for VC are focused on maintaining calcium and phosphorus

483   homeostasis. Traditionally drug development has relied on physical experiments and

484   drug compounds, but adding indications to existing drugs to treat other diseases is a

485   valid alternative. For example, sildenafil (Viagra) was initially used to treat angina but is

486   now used to treat erectile dysfunction. Using the Dgidb database, we screened 16 drugs

487   targeting these central genes, some for the treatment of VC and some for other

488   diseases. Insulin has been reported to attenuate calcification of vascular smooth muscle

489   sarcomeres(Wang et al. 2007). Romosozumab is used for the treatment of osteoporosis

490   in women(Turk et al. 2020). I19-IL2 selectively activates Tregs to eliminate local

491   inflammation and induce plaque shrinkage in mice, thereby inhibiting atherosclerotic

492   plaques (Dietrich et al. 2012). The results of probability score selection suggest that

493   daidzein as an antioxidant may attenuate VC (Chao et al. 2022). Wortmannin may treat

494   VC by inhibiting phosphatidylinositol 3-kinase-related DDR1 (Lino et al. 2018).

495   Tacrolimus immunosuppression has a therapeutic effect on bone loss and the tendency

496 of cyclosporine A to cause vascular disease(Hofbauer et al. 2001). Immune, antioxidant,

497 and phosphatidylinositol 3-kinase inhibition pathways may be investigated as a

498 treatment for VC, complementing the traditional therapeutic approach of maintaining

499 calcium and phosphorus homeostasis. However, more basic research and clinical trials

500 are needed in the future to verify how effective these drugs are in treating VC and

501 whether they cause side effects.

502

503 However, there are still some limitations of our study. First, due to the lack of other

504 vascular calcification datasets, it was impossible to validate our analysis results using

505 different datasets. Second, although we constructed a vascular calcification model to

506 validate the expression levels of hub genes, the validity of the final analysis results

507 needs to be verified in human tissues due to species differences. Third, although we

508 have used bioinformatics methods to preliminarily analyze the gene sets involved in VC,

509 the connection of these gene sets with actual biology needs further experimental proof.

510

511 **_Conclusions_**

512 In conclusion, through bioinformatics analysis and experimental validation, we found

513 that these hub genes (Spp1, Sost, Col1a1, Fn1, Ibsp) are consistently present and play

514 a regulatory role throughout the progression of VC. These hub genes can act as

515 biomarkers for the diagnosis and treatment of VC.

516

517 ***Funding Statement***

518 This work was supported by The National Natural Science Foundation of China (No:

519 81960091).

520

Additional Information and Declarations

522 Competing Interests

523 The authors declare that they have no competing interests.

524

525 Author Contributions

526 Chuanzhen Chen conceived and designed the experiments, performed the

527 experiments, analyzed the data, prepared figures and/or tables, authored or reviewed

528 drafts of the paper, and approved the final draft.

529 Yinteng Wu conceived and designed the experiments, authored or reviewed drafts of

530 the paper, and approved the final draft.

531 Hailin Lu conceived and designed the experiments, authored or reviewed drafts of the

532 paper, and approved the final draft.

533 Kai Liu conceived and designed the experiments, authored or reviewed drafts of the

534 paper, and approved the final draft.

535 Xiao Qin conceived and designed the experiments, analyzed the data, prepared figures

536 and/or tables, authored or reviewed drafts of the paper, and approved the final draft.

537 All authors contributed equally to this work.

538

539 ***References***

540 Ayari H, and Bricca G. 2012. Microarray analysis reveals overexpression of IBSP in

541   human carotid plaques. Adv Med Sci 57:334-340. 10.2478/v10039-012-0056-0

542 Bell J. 2004. Predicting disease using genomics. Nature 429:453-456.

543   10.1038/nature02624

544 Bostom A, Pasch A, Madsen T, Roberts MB, Franceschini N, Steubl D, Garimella PS, Ix

545   JH, Tuttle KR, Ivanova A, Shireman T, Gohh R, Merhi B, Jarolim P, Kusek JW,

546   Pfeffer MA, Liu S, and Eaton CB. 2018. Serum Calcification Propensity and Fetuin-

547   A: Biomarkers of Cardiovascular Disease in Kidney Transplant Recipients. *Am J*

548   *Nephrol* 48:21-31. 10.1159/000491025

549 Budoff MJ, Hokanson JE, Nasir K, Shaw LJ, Kinney GL, Chow D, Demoss D, Nuguri V,

550   Nabavi V, Ratakonda R, Berman DS, and Raggi P. 2010. Progression of coronary

551   artery calcium predicts all-cause mortality. *JACC Cardiovasc Imaging* 3:1229-

552   1236. 10.1016/j.jcmg.2010.08.018

553 Catalano A, Bellone F, Morabito N, and Corica F. 2020. Sclerostin and Vascular

554   Pathophysiology. *Int J Mol Sci* 21. 10.3390/ijms21134779

555 Chang Z, Yan G, Zheng J, and Liu Z. 2020. The lncRNA GAS5 Inhibits the Osteogenic

556   Differentiation and Calcification of Human Vascular Smooth Muscle Cells. *Calcif*

557    *Tissue Int* 107:86-95. 10.1007/s00223-020-00696-1

558 Chao CT, Tsai YT, Lee WT, Yeh HY, and Chiang CK. 2022. Deep Learning-Assisted

559    Repurposing of Plant Compounds for Treating Vascular Calcification: An In Silico

560    Study with Experimental Validation. *Oxid Med Cell Longev* 2022:4378413.

561    10.1155/2022/4378413

562 Chen Y, Zhao X, and Wu H. 2020. Arterial Stiffness: A Focus on Vascular Calcification

563    and Its Link to Bone Mineralization. *Arterioscler Thromb Vasc Biol* 40:1078-1093.

564    10.1161/atvbaha.120.313131

565 Cheng SL, Shao JS, Halstead LR, Distelhorst K, Sierra O, and Towler DA. 2010.

566    Activation of vascular smooth muscle parathyroid hormone receptor inhibits

567    Wnt/beta-catenin signaling and aortic fibrosis in diabetic arteriosclerosis. *Circ Res*

568    107:271-282. 10.1161/circresaha.110.219899

569 Chistiakov DA, Sobenin IA, and Orekhov AN. 2013. Vascular extracellular matrix in

570    atherosclerosis. *Cardiol Rev* 21:270-288. 10.1097/CRD.0b013e31828c5ced

571 Choe N, Kwon DH, Ryu J, Shin S, Cho HJ, Joung H, Eom GH, Ahn Y, Park WJ, Nam KI,

572    Kim YK, and Kook H. 2020a. miR-27a-3p Targets ATF3 to Reduce Calcium

573    Deposition in Vascular Smooth Muscle Cells. *Mol Ther Nucleic Acids* 22:627-639.

574    10.1016/j.omtn.2020.09.030

575 Choe N, Shin S, Joung H, Ryu J, Kim YK, Ahn Y, Kook H, and Kwon DH. 2020b. The

576    microRNA miR-134-5p induces calcium deposition by inhibiting histone

577   deacetylase 5 in vascular smooth muscle cells. *J Cell Mol Med* 24:10542-10550.

578   10.1111/jcmm.15670

579 Cong J, Cheng B, Liu J, and He P. 2021. RTEF-1 Inhibits Vascular Smooth Muscle Cell

580   Calcification through Regulating Wnt/β-Catenin Signaling Pathway. *Calcif Tissue*

581   *Int* 109:203-214. 10.1007/s00223-021-00833-4

582 Cui L, Zhou Q, Zheng X, Sun B, and Zhao S. 2020. Mitoquinone attenuates vascular

583   calcification by suppressing oxidative stress and reducing apoptosis of vascular

584   smooth muscle cells via the Keap1/Nrf2 pathway. *Free Radic Biol Med* 161:23-31.

585   10.1016/j.freeradbiomed.2020.09.028

586 De Maré A, Maudsley S, Azmi A, Hendrickx JO, Opdebeeck B, Neven E, D'Haese PC,

587   and Verhulst A. 2019. Sclerostin as Regulatory Molecule in Vascular Media

588   Calcification and the Bone-Vascular Axis. *Toxins (Basel)* 11.

589   10.3390/toxins11070428

590 Deng L, Huang L, Sun Y, Heath JM, Wu H, and Chen Y. 2015. Inhibition of FOXO1/3

591   promotes vascular calcification. *Arterioscler Thromb Vasc Biol* 35:175-183.

592   10.1161/atvbaha.114.304786

593 Dietrich T, Hucko T, Schneemann C, Neumann M, Menrad A, Willuda J, Atrott K, Stibenz

594   D, Fleck E, Graf K, and Menssen HD. 2012. Local delivery of IL-2 reduces

595   atherosclerosis via expansion of regulatory T cells. *Atherosclerosis* 220:329-336.

596   10.1016/j.atherosclerosis.2011.09.050

597 Ding HT, Wang CG, Zhang TL, and Wang K. 2006. Fibronectin enhances in vitro vascular

598   calcification by promoting osteoblastic differentiation of vascular smooth muscle

599   cells via ERK pathway. *J Cell Biochem* 99:1343-1352. 10.1002/jcb.20999

600 Doherty TM, Asotra K, Fitzpatrick LA, Qiao JH, Wilkin DJ, Detrano RC, Dunstan CR, Shah

601   PK, and Rajavashisth TB. 2003. Calcification in atherosclerosis: bone biology and

602   chronic inflammation at the arterial crossroads. *Proc Natl Acad Sci U S A*

603   100:11201-11206. 10.1073/pnas.1932554100

604 Downes K, Megy K, Duarte D, Vries M, Gebhart J, Hofer S, Shamardina O, Deevi SVV,

605   Stephens J, Mapeta R, Tuna S, Al Hasso N, Besser MW, Cooper N, Daugherty L,

606   Gleadall N, Greene D, Haimel M, Martin H, Papadia S, Revel-Vilk S,

607   Sivapalaratnam S, Symington E, Thomas W, Thys C, Tolios A, Penkett CJ,

608   Ouwehand WH, Abbs S, Laffan MA, Turro E, Simeoni I, Mumford AD, Henskens

609   YMC, Pabinger I, Gomez K, and Freson K. 2019. Diagnostic high-throughput

610   sequencing of 2396 patients with bleeding, thrombotic, and platelet disorders.

611   *Blood* 134:2082-2091. 10.1182/blood.2018891192

612 Duer M, Cobb AM, and Shanahan CM. 2020. DNA Damage Response: A Molecular

613   Lynchpin in the Pathobiology of Arteriosclerotic Calcification. *Arterioscler Thromb*

614   *Vasc Biol* 40:e193-e202. 10.1161/ATVBAHA.120.313792

615 Durham AL, Speer MY, Scatena M, Giachelli CM, and Shanahan CM. 2018. Role of

616   smooth muscle cells in vascular calcification: implications in atherosclerosis and

617   arterial stiffness. *Cardiovasc Res* 114:590-600. 10.1093/cvr/cvy010

618 El-Maadawy S, Kaartinen MT, Schinke T, Murshed M, Karsenty G, and McKee MD. 2003.

619   Cartilage formation and calcification in arteries of mice lacking matrix Gla protein.

620   *Connect Tissue Res* 44 Suppl 1:272-278.

621 Ferrer MD, Ketteler M, Tur F, Tur E, Isern B, Salcedo C, Joubert PH, Behets GJ, Neven

622   E, D'Haese PC, and Perelló J. 2018. Characterization of SNF472

623   pharmacokinetics and efficacy in uremic and non-uremic rats models of

624   cardiovascular calcification. *PLoS One* 13:e0197061.

625   10.1371/journal.pone.0197061

626 Foresta C, Strapazzon G, De Toni L, Fabris F, Grego F, Gerosa G, Vettore S, and Garolla

627   A. 2013. Platelets express and release osteocalcin and co-localize in human

628   calcified atherosclerotic plaques. *J Thromb Haemost* 11:357-365.

629   10.1111/jth.12088

630 Giachelli CM. 2004. Mechanisms of vascular calcification in uremia. *Semin Nephrol*

631   24:401-402. 10.1016/j.semnephrol.2004.06.005

632 Giger EV, Castagner B, and Leroux JC. 2013. Biomedical applications of

633   bisphosphonates. *J Control Release* 167:175-188. 10.1016/j.jconrel.2013.01.032

634 Green ED, Watson JD, and Collins FS. 2015. Human Genome Project: Twenty-five years

635   of big biology. *Nature* 526:29-31. 10.1038/526029a

636 Hofbauer LC, Shui C, Riggs BL, Dunstan CR, Spelsberg TC, O'Brien T, and Khosla S.

637   2001. Effects of immunosuppressants on receptor activator of NF-kappaB ligand

638   and osteoprotegerin production by human osteoblastic and coronary artery smooth

639   muscle cells. *Biochem Biophys Res Commun* 280:334-339.

640   10.1006/bbrc.2000.4130

641 Hsu JJ, Lim J, Tintut Y, and Demer LL. 2016. Cell-matrix mechanics and pattern formation

642   in inflammatory cardiovascular calcification. *Heart* 102:1710-1715.

643   10.1136/heartjnl-2016-309667

644 Iqbal F, Lupieri A, Aikawa M, and Aikawa E. 2021. Harnessing Single-Cell RNA

645   Sequencing to Better Understand How Diseased Cells Behave the Way They Do

646   in Cardiovascular Disease. *Arterioscler Thromb Vasc Biol* 41:585-600.

647   10.1161/atvbaha.120.314776

648 Jacob MP. 2003. Extracellular matrix remodeling and matrix metalloproteinases in the

649   vascular wall during aging and in pathological conditions. *Biomed Pharmacother*

650   57:195-202. 10.1016/s0753-3322(03)00065-9

651 Jiang W, Zhang Z, Li Y, Chen C, Yang H, Lin Q, Hu M, and Qin X. 2021. The Cell Origin

652   and Role of Osteoclastogenesis and Osteoblastogenesis in Vascular Calcification.

653   *Front Cardiovasc Med* 8:639740. 10.3389/fcvm.2021.639740

654 Jiang W, Zhang Z, Yang H, Lin Q, Han C, and Qin X. 2017. The Involvement of miR-29b-

655   3p in Arterial Calcification by Targeting Matrix Metalloproteinase-2. *Biomed Res*

656   *Int* 2017:6713606. 10.1155/2017/6713606

657 Kapetanios D, Karkos C, Giagtzidis I, Papazoglou K, Kiroplastis K, and Spyridis C. 2016.

658   Vascular calcification biomarkers and peripheral arterial disease. *Int Angiol*

659   35:455-459.

660 Khundmiri SJ, Murray RD, and Lederer E. 2016. PTH and Vitamin D. *Compr Physiol*

661   6:561-601. 10.1002/cphy.c140071

662 Lacolley P, Regnault V, Segers P, and Laurent S. 2017. Vascular Smooth Muscle Cells

663   and Arterial Stiffening: Relevance in Development, Aging, and Disease. *Physiol*

664   *Rev* 97:1555-1617. 10.1152/physrev.00003.2017

665 Lee SJ, Lee IK, and Jeon JH. 2020. Vascular Calcification-New Insights Into Its

666   Mechanism. *Int J Mol Sci* 21. 10.3390/ijms21082685

667 Leopold JA. 2015. Vascular calcification: Mechanisms of vascular smooth muscle cell

668   calcification. *Trends Cardiovasc Med* 25:267-274. 10.1016/j.tcm.2014.10.021

669 Liberman M, Johnson RC, Handy DE, Loscalzo J, and Leopold JA. 2011. Bone

670   morphogenetic protein-2 activates NADPH oxidase to increase endoplasmic

671   reticulum stress and human coronary artery smooth muscle cell calcification.

672   *Biochem Biophys Res Commun* 413:436-441. 10.1016/j.bbrc.2011.08.114

673 Lindholt JS, Frystyk J, Hallas J, Rasmussen LM, and Diederichsen ACP. 2020. Feasibility

674   Study of Advanced Cardiovascular Screening in Middle-Aged Patients with

675   Diabetes. *Clin Epidemiol* 12:447-455. 10.2147/clep.S246636

676 Lino M, Wan MH, Rocca AS, Ngai D, Shobeiri N, Hou G, Ge C, Franceschi RT, and

677   Bendeck MP. 2018. Diabetic Vascular Calcification Mediated by the Collagen

678   Receptor Discoidin Domain Receptor 1 via the Phosphoinositide 3-

679   Kinase/Akt/Runt-Related Transcription Factor 2 Signaling Axis. *Arterioscler*

680   *Thromb Vasc Biol* 38:1878-1889. 10.1161/atvbaha.118.311238

681 Lomashvili KA, Monier-Faugere MC, Wang X, Malluche HH, and O'Neill WC. 2009. Effect

682 of bisphosphonates on vascular calcification and bone metabolism in experimental

683 renal failure. *Kidney Int* 75:617-625. 10.1038/ki.2008.646

684 London GM, Guérin AP, Marchais SJ, Métivier F, Pannier B, and Adda H. 2003. Arterial

685 media calcification in end-stage renal disease: impact on all-cause and

686 cardiovascular mortality. *Nephrol Dial Transplant* 18:1731-1740.

687 10.1093/ndt/gfg414

688 Luo G, Ducy P, McKee MD, Pinero GJ, Loyer E, Behringer RR, and Karsenty G. 1997.

689 Spontaneous calcification of arteries and cartilage in mice lacking matrix GLA

690 protein. *Nature* 386:78-81. 10.1038/386078a0

691 Martínez-López D, Roldan-Montero R, García-Marqués F, Nuñez E, Jorge I, Camafeita

692 E, Minguez P, Rodriguez de Cordoba S, López-Melgar B, Lara-Pezzi E,

693 Fernández-Ortiz A, Ibáñez B, Valdivielso JM, Fuster V, Michel JB, Blanco-Colio

694 LM, Vázquez J, and Martin-Ventura JL. 2020. Complement C5 Protein as a Marker

695 of Subclinical Atherosclerosis. *J Am Coll Cardiol* 75:1926-1941.

696 10.1016/j.jacc.2020.02.058

697 Massy ZA, Mentaverri R, Mozar A, Brazier M, and Kamel S. 2008. The pathophysiology

698 of vascular calcification: are osteoclast-like cells the missing link? *Diabetes Metab*

699 34 Suppl 1:S16-20. 10.1016/s1262-3636(08)70098-3

700 Mizobuchi M, Towler D, and Slatopolsky E. 2009. Vascular calcification: the killer of

701 patients with chronic kidney disease. *J Am Soc Nephrol* 20:1453-1464.

702 10.1681/asn.2008070692

703   Paloian NJ, Leaf EM, and Giachelli CM. 2016. Osteopontin protects against high

704   phosphate-induced nephrocalcinosis and vascular calcification. *Kidney Int*

705   89:1027-1036. 10.1016/j.kint.2015.12.046

706   Pescatore LA, Gamarra LF, and Liberman M. 2019. Multifaceted Mechanisms of Vascular

707   Calcification in Aging. *Arterioscler Thromb Vasc Biol* 39:1307-1316.

708   10.1161/atvbaha.118.311576

709   Pilz S, Verheyen N, Grübler MR, Tomaschitz A, and März W. 2016. Vitamin D and

710   cardiovascular disease prevention. *Nat Rev Cardiol* 13:404-417.

711   10.1038/nrcardio.2016.73

712   Pressman GS, Rodriguez-Ziccardi M, Gartman CH, Obasare E, Melendres E, Arguello V,

713   and Bhalla V. 2017. Mitral Annular Calcification as a Possible Nidus for

714   Endocarditis: A Descriptive Series with Bacteriological Differences Noted. *J Am*

715   *Soc Echocardiogr* 30:572-578. 10.1016/j.echo.2017.01.016

716   Rukov JL, Gravesen E, Mace ML, Hofman-Bang J, Vinther J, Andersen CB, Lewin E, and

717   Olgaard K. 2016. Effect of chronic uremia on the transcriptional profile of the

718   calcified aorta analyzed by RNA sequencing. *Am J Physiol Renal Physiol*

719   310:F477-491. 10.1152/ajprenal.00472.2015

720   Rung J, and Brazma A. 2013. Reuse of public genome-wide gene expression data. *Nat*

721   *Rev Genet* 14:89-99. 10.1038/nrg3394

722   Ryu J, Choe N, Kwon DH, Shin S, Lim YH, Yoon G, Kim JH, Kim HS, Lee IK, Ahn Y, Park

723   WJ, Kook H, and Kim YK. 2022. Circular RNA circSmoc1-2 regulates vascular

724   calcification by acting as a miR-874-3p sponge in vascular smooth muscle cells.

725   *Mol Ther Nucleic Acids* 27:645-655. 10.1016/j.omtn.2021.12.031

726 Schlieper G, Brandenburg V, Ketteler M, and Floege J. 2009. Sodium thiosulfate in the

727   treatment of calcific uremic arteriolopathy. *Nat Rev Nephrol* 5:539-543.

728   10.1038/nrneph.2009.99

729 Scialla JJ, Leonard MB, Townsend RR, Appel L, Wolf M, Budoff MJ, Chen J, Lustigova

730   E, Gadegbeku CA, Glenn M, Hanish A, Raj D, Rosas SE, Seliger SL, Weir MR,

731   and Parekh RS. 2011. Correlates of osteoprotegerin and association with aortic

732   pulse wave velocity in patients with chronic kidney disease. *Clin J Am Soc Nephrol*

733   6:2612-2619. 10.2215/cjn.03910411

734 Shea MK, and Booth SL. 2019. Vitamin K, Vascular Calcification, and Chronic Kidney

735   Disease: Current Evidence and Unanswered Questions. *Curr Dev Nutr* 3:nzz077.

736   10.1093/cdn/nzz077

737 Shroff R, Long DA, and Shanahan C. 2013. Mechanistic insights into vascular calcification

738   in CKD. *J Am Soc Nephrol* 24:179-189. 10.1681/asn.2011121191

739 Shroff RC, McNair R, Figg N, Skepper JN, Schurgers L, Gupta A, Hiorns M, Donald AE,

740   Deanfield J, Rees L, and Shanahan CM. 2008. Dialysis accelerates medial

741   vascular calcification in part by triggering smooth muscle cell apoptosis. *Circulation*

742   118:1748-1757. 10.1161/circulationaha.108.783738

743 Singh A, Tandon S, and Tandon C. 2021. An update on vascular calcification and

744   potential therapeutics. *Mol Biol Rep* 48:887-896. 10.1007/s11033-020-06086-y

745 Strauss HW, Nakahara T, Narula N, and Narula J. 2019. Vascular Calcification: The

746   Evolving Relationship of Vascular Calcification to Major Acute Coronary Events. *J*

747   *Nucl Med* 60:1207-1212. 10.2967/jnumed.119.230276

748 Towler DA, Shao JS, Cheng SL, Pingsterhaus JM, and Loewy AP. 2006. Osteogenic

749   regulation of vascular calcification. *Ann N Y Acad Sci* 1068:327-333.

750   10.1196/annals.1346.036

751 Turk JR, Deaton AM, Yin J, Stolina M, Felx M, Boyd G, Bienvenu JG, Varela A, Guillot M,

752   Holdsworth G, Wolfreys A, Dwyer D, Kumar SV, de Koning EM, Qu Y, Engwall M,

753   Locher K, Ward LD, Glaus C, He YD, and Boyce RW. 2020. Nonclinical

754   cardiovascular safety evaluation of romosozumab, an inhibitor of sclerostin for the

755   treatment of osteoporosis in postmenopausal women at high risk of fracture. *Regul*

756   *Toxicol Pharmacol* 115:104697. 10.1016/j.yrtph.2020.104697

757 Uto K, Yoshizawa S, Aoki C, Nishikawa T, and Oda H. 2021. Inhibition of extracellular

758   matrix integrity attenuates the early phase of aortic medial calcification in a rodent

759   model. *Atherosclerosis* 319:10-20. 10.1016/j.atherosclerosis.2020.12.015

760 Valenti V, Hartaigh B, Cho I, Schulman-Marcus J, Gransar H, Heo R, Truong QA, Shaw

761   LJ, Knapper J, Kelkar AA, Sciarretta S, Chang HJ, Callister TQ, and Min JK. 2016.

762   Absence of Coronary Artery Calcium Identifies Asymptomatic Diabetic Individuals

763   at Low Near-Term But Not Long-Term Risk of Mortality: A 15-Year Follow-Up

764   Study of 9715 Patients. *Circ Cardiovasc Imaging* 9:e003528.

765   10.1161/circimaging.115.003528

766 Van Campenhout A, and Golledge J. 2009. Osteoprotegerin, vascular calcification and

767   atherosclerosis. *Atherosclerosis* 204:321-329.

768   10.1016/j.atherosclerosis.2008.09.033

769 Vogelstein B, Papadopoulos N, Velculescu VE, Zhou S, Diaz LA, Jr., and Kinzler KW.

770   2013. Cancer genome landscapes. *Science* 339:1546-1558.

771   10.1126/science.1235122

772 Wang CC, Sorribas V, Sharma G, Levi M, and Draznin B. 2007. Insulin attenuates

773   vascular smooth muscle calcification but increases vascular smooth muscle cell

774   phosphate transport. *Atherosclerosis* 195:e65-75.

775   10.1016/j.atherosclerosis.2007.02.032

776 Wheeler DA, and Wang L. 2013. From human genome to cancer genome: the first

777   decade. *Genome Res* 23:1054-1062. 10.1101/gr.157602.113

778 Yao Y, Yao J, and Boström KI. 2019. SOX Transcription Factors in Endothelial

779   Differentiation and Endothelial-Mesenchymal Transitions. *Front Cardiovasc Med*

780   6:30. 10.3389/fcvm.2019.00030

781 Yoshida T, Yamashita M, and Hayashi M. 2012. Kruppel-like factor 4 contributes to high

782   phosphate-induced phenotypic switching of vascular smooth muscle cells into

783   osteogenic cells. *J Biol Chem* 287:25706-25714. 10.1074/jbc.M112.361360

784 Zhang B, Zhang G, Wei T, Yang Z, Tan W, Mo Z, Liu J, Li D, Wei Y, Zhang L, Webster

785   KA, and Wei J. 2019. MicroRNA-25 Protects Smooth Muscle Cells against

786   Corticosterone-Induced Apoptosis. *Oxid Med Cell Longev* 2019:2691514.

787   10.1155/2019/2691514

788   Zhang Z, Zhang X, Wang C, Zhou P, Xiao J, Zheng H, Wang L, Yan S, Zhang Y, and Ji

789   X. 2021. Deacetylated Sp1 improves β-glycerophosphate-induced calcification in

790   vascular smooth muscle cells. *Exp Ther Med* 22:1152. 10.3892/etm.2021.10586

791

792
793

Figure 1

Research flow chart.
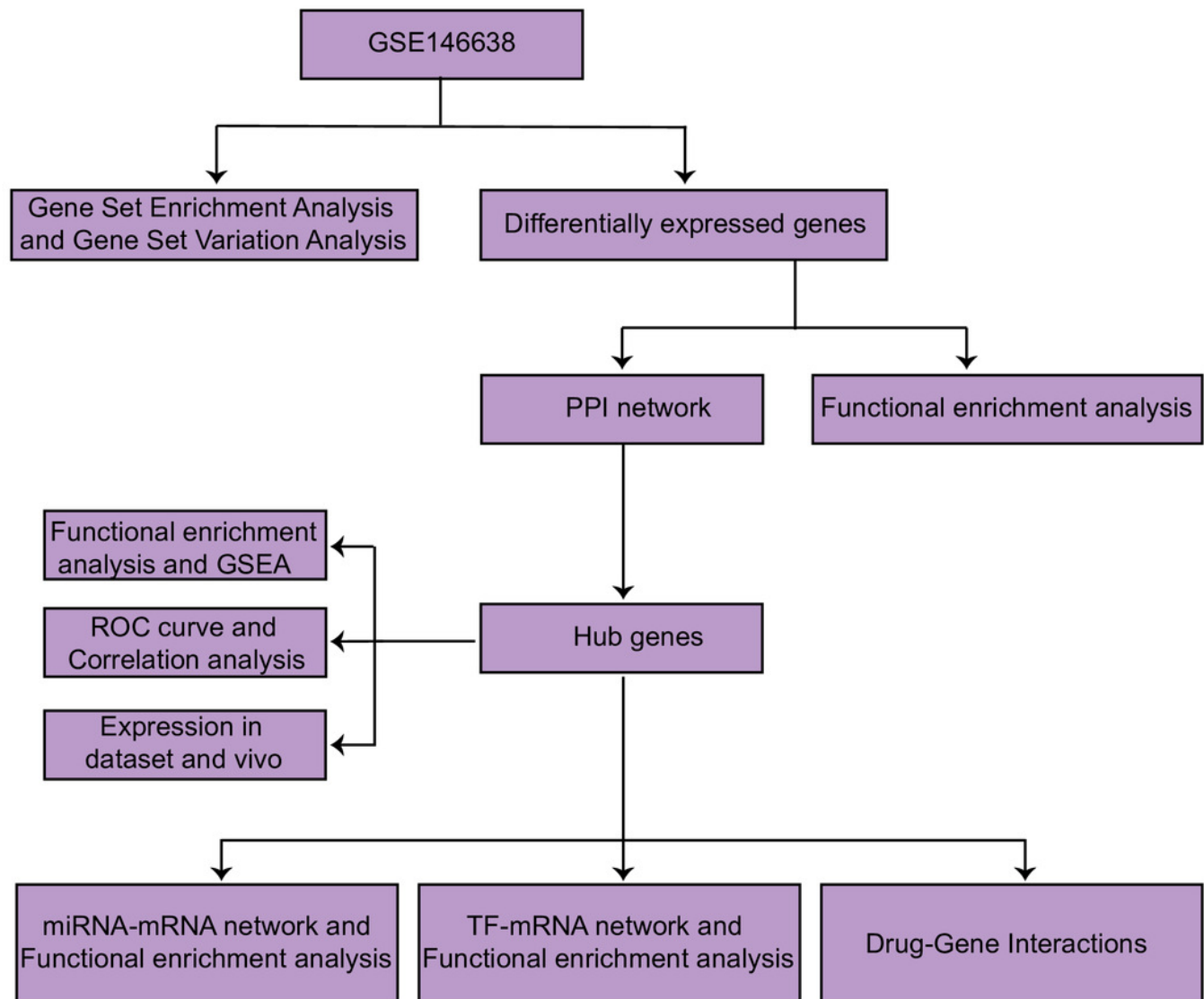
Figure 2

Screening of DEGs.

(A) Volcano plot of DEGs between uremia-induced vascular calcified samples and normal control samples. (B) Volcano plot of DEGs between vitamin D3-induced vascular calcified samples and normal control samples. Red dots: genes significantly up-regulated in VC. Gray-green dots: genes significantly down-regulated in VC; black dots: genes not differentially expressed. |log2FC|>1 and FDR<0.05 as cutoff criteria. (C) The Venn diagram of down-regulated DEGs with different degrees of vascular calcification. (D) The Venn diagram of up-regulated DEGs with different degrees of VC.

A

GSE146638-Uremia-VC to Control

B

GSE146638-Vitamin D3-VC to Control
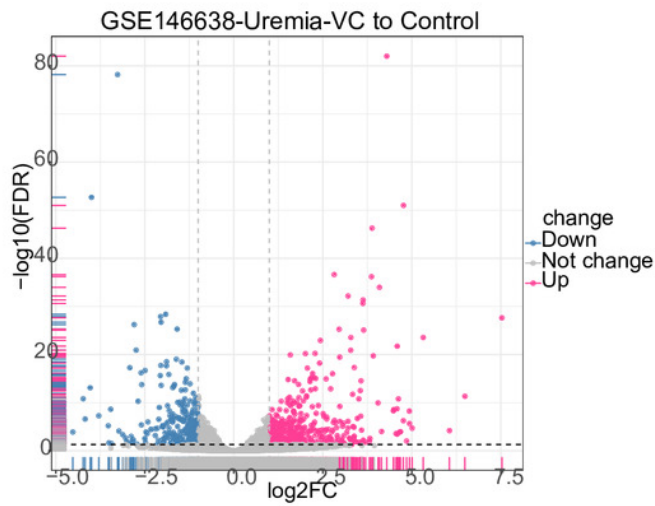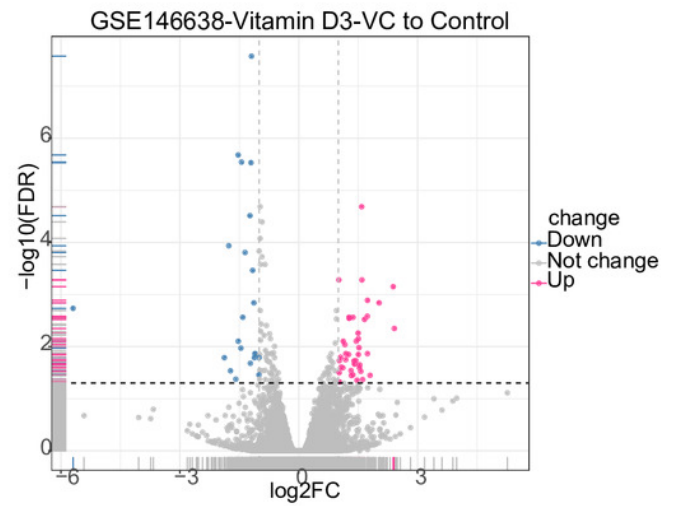
C
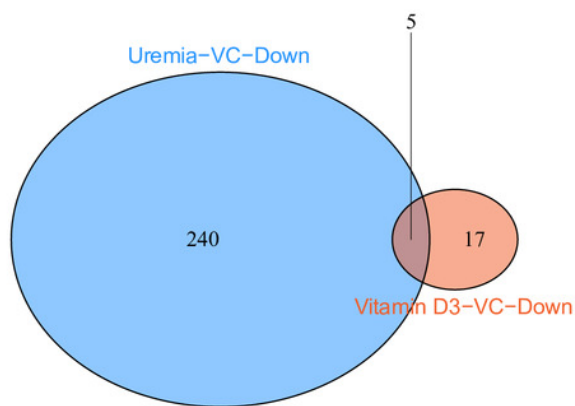
D
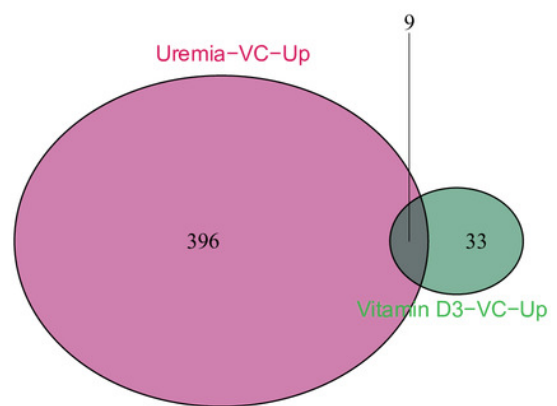
Figure 3

The GESE between the uremia-induced VC group and the normal group.

The GSEA includes GO BP analysis (A), GO CC analysis (B), GO MF analysis (C), and KEGG pathway analysis (D).
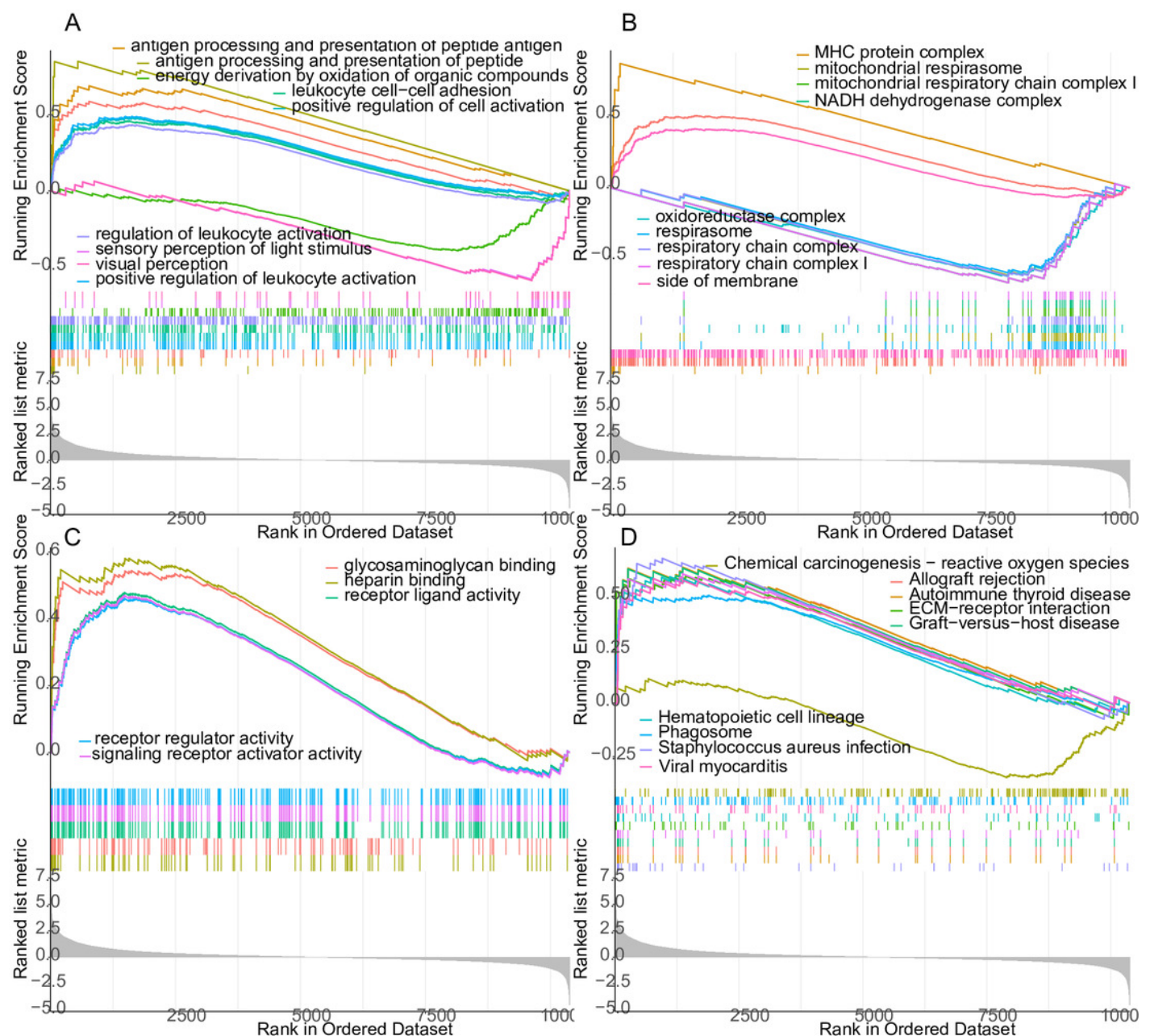
Figure 4

The GSVA between the uremia-induced VC group and the normal group.

The GSVA includes GO analysis (A) and KEGG pathway analysis (B).
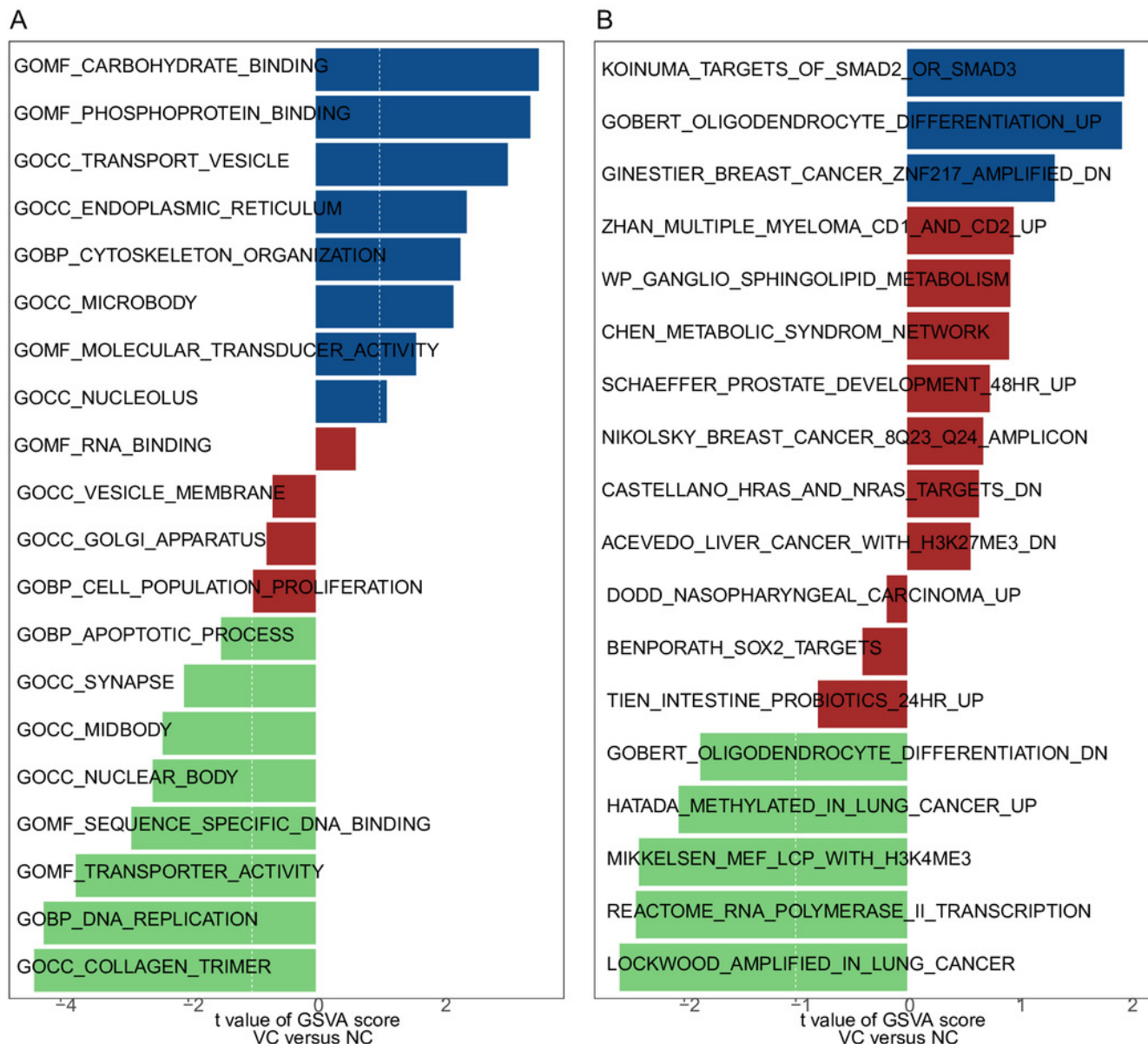
Figure 5

Functional enrichment analysis and pathway of DEGs.

(A) GO BP analysis. (B) GO CC analysis. (C) GO MF analysis. (D) KEGG pathway analysis.
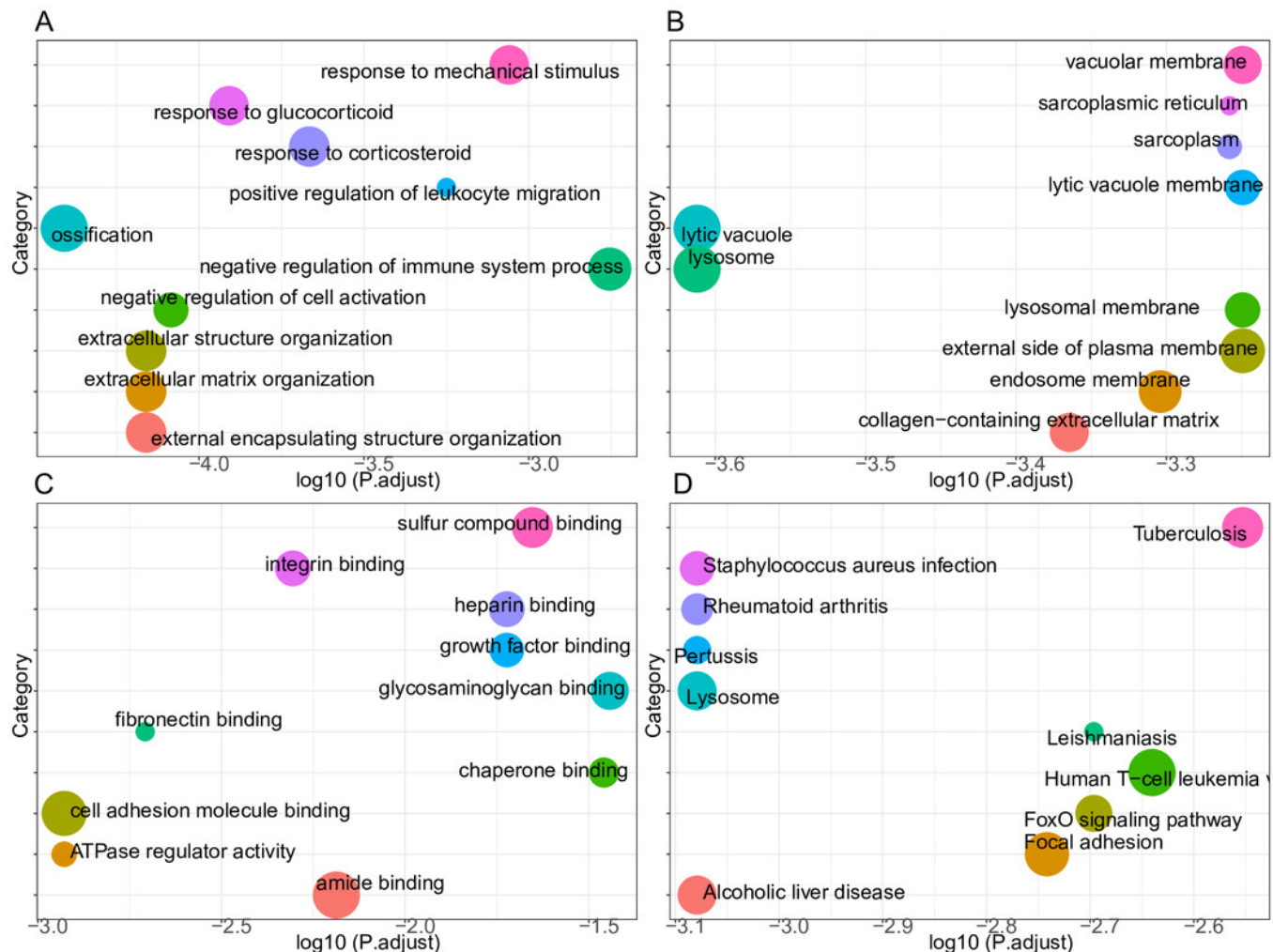
Figure 6

PPI network construction, hub genes functional enrichment analysis and correlation.

PPI network construction, hub genes functional enrichment analysis and correlation. (A) The PPI network of DEGs in the uremic-induced VC group. (B) The PPI network of DEGs in the vitamin D3-induced VC group. (C) The PPI network of the intersection of two DEGs with different degrees of calcification. (D) Functional enrichment analysis and pathway analysis of hub genes. (E) The correlations between hub genes. (F) The functional similarities between hub genes.

A

B

C

D

BP
GO:0001503: ossification
GO:0048545: steroid hormone
GO:0009612: mechanical stimulus
GO:0001944: vasculature development

CC
GO:0031012: extracellular matrix
-log10(P)

MF
GO:0050839: cell adhesion molecule binding
GO:0005178: integrin binding
-log10(P)

KEGG
ko04512: ECM-receptor interaction
-log10(P)
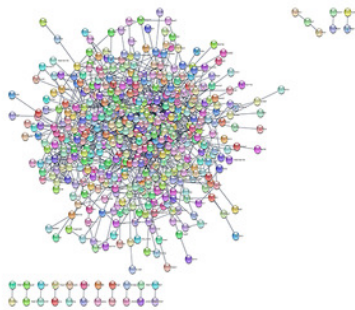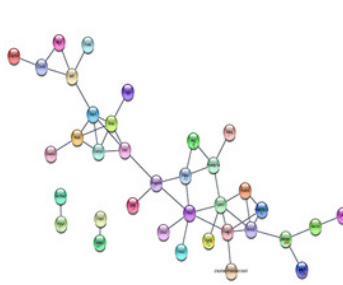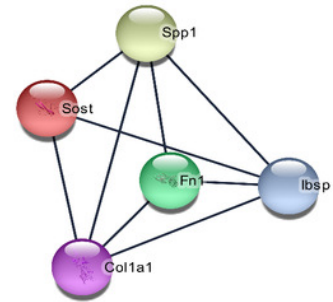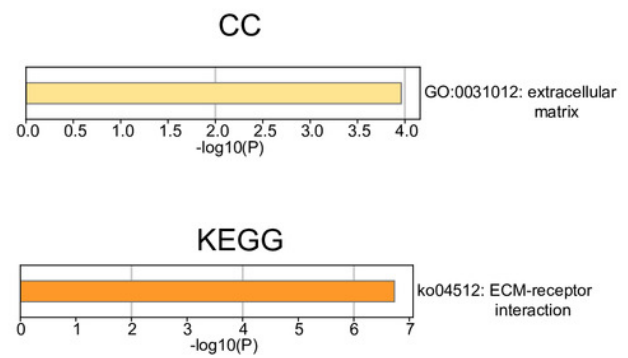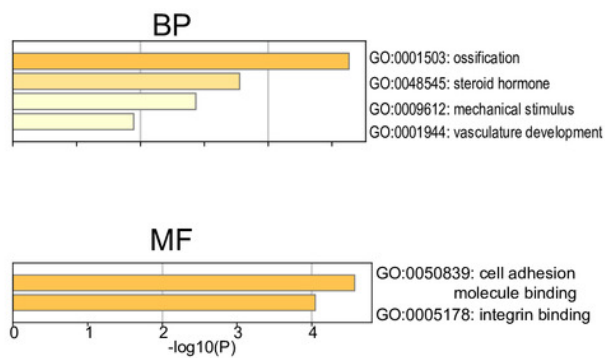
E
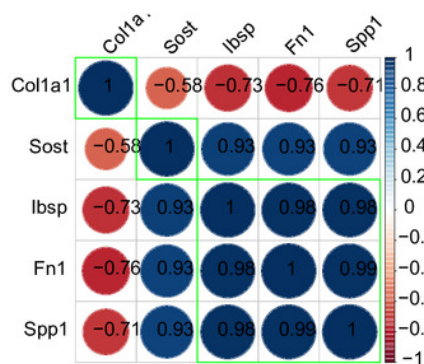
F
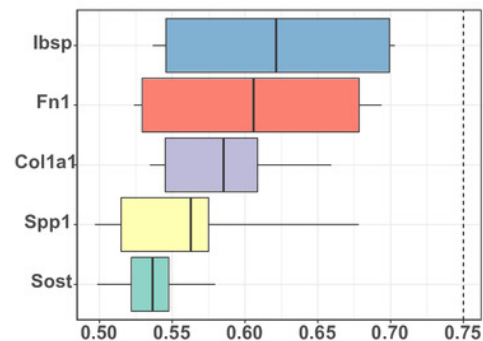
Figure 7

ROC curves and expression of hub genes in the dataset.

(A) The ROC curve of each hub gene in uremia-induced VC samples was compared with normal vessels. (B) The expression of each hub gene in uremia-induced VC samples was compared with normal vessels.

A
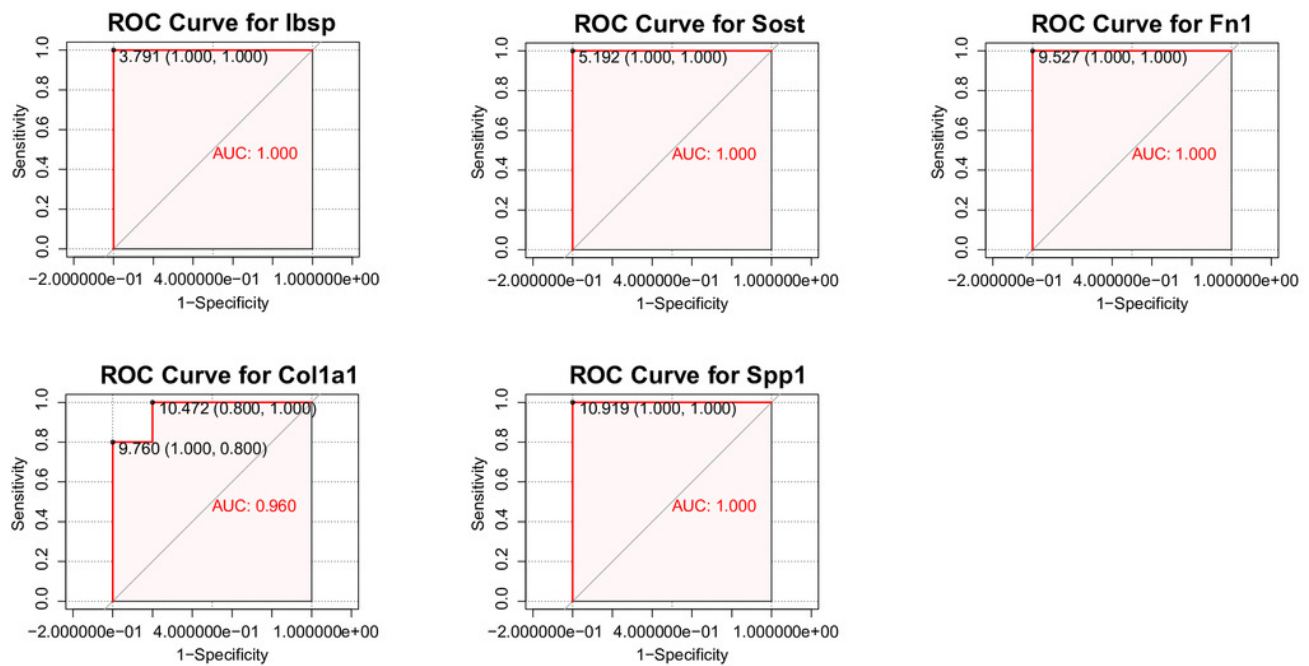
B
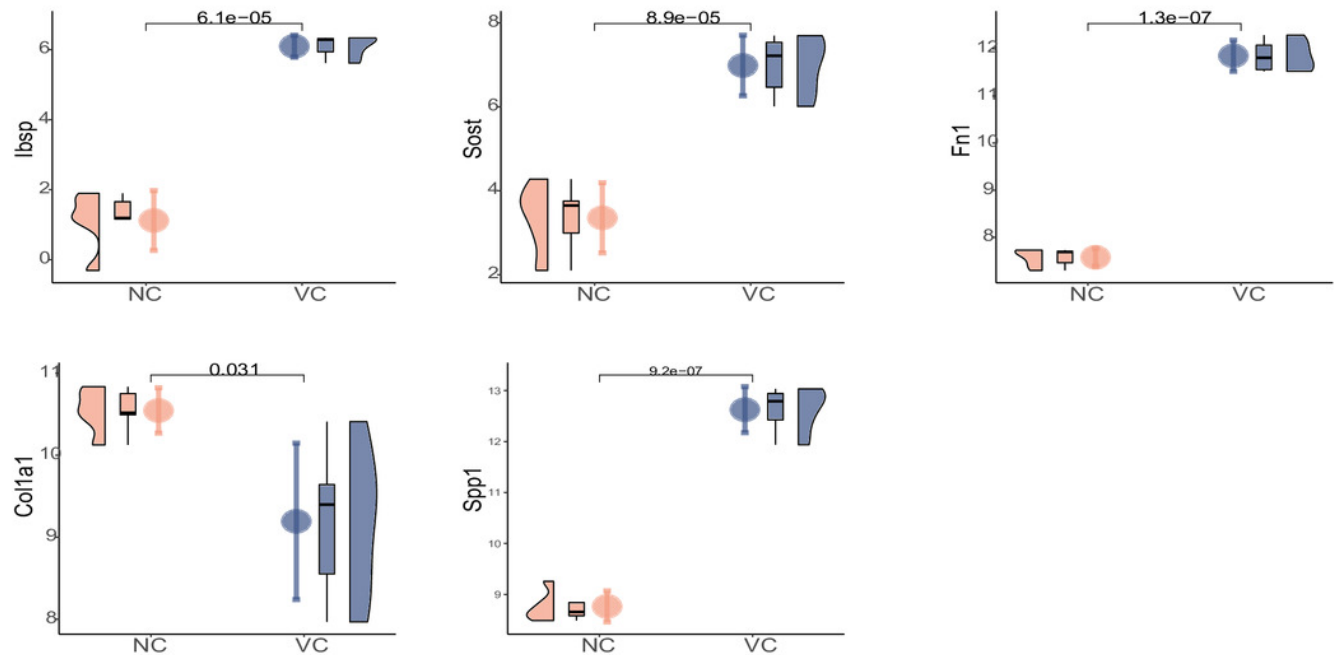
Figure 8

Validation of each hub gene expression in rat aorta with VC.

(A) Alizarin red staining and Von Kossa staining of rat aorta. The positively stained regions were analyzed using ImageJ. The scale bar represents 500 um (black) and 200 um (red). (B) Relative expression in RT-qPCR of these hub genes. (C) The expression of hub genes in the thoracic artery were detected by immunohistochemistry and the average optical density values were analyzed by ImageJ. The scale bar represents 500 μm (black) and 100 μm (green). *$P<0.05$, **$P<0.01$, ***$P<0.001$, ****$P<0.0001$.
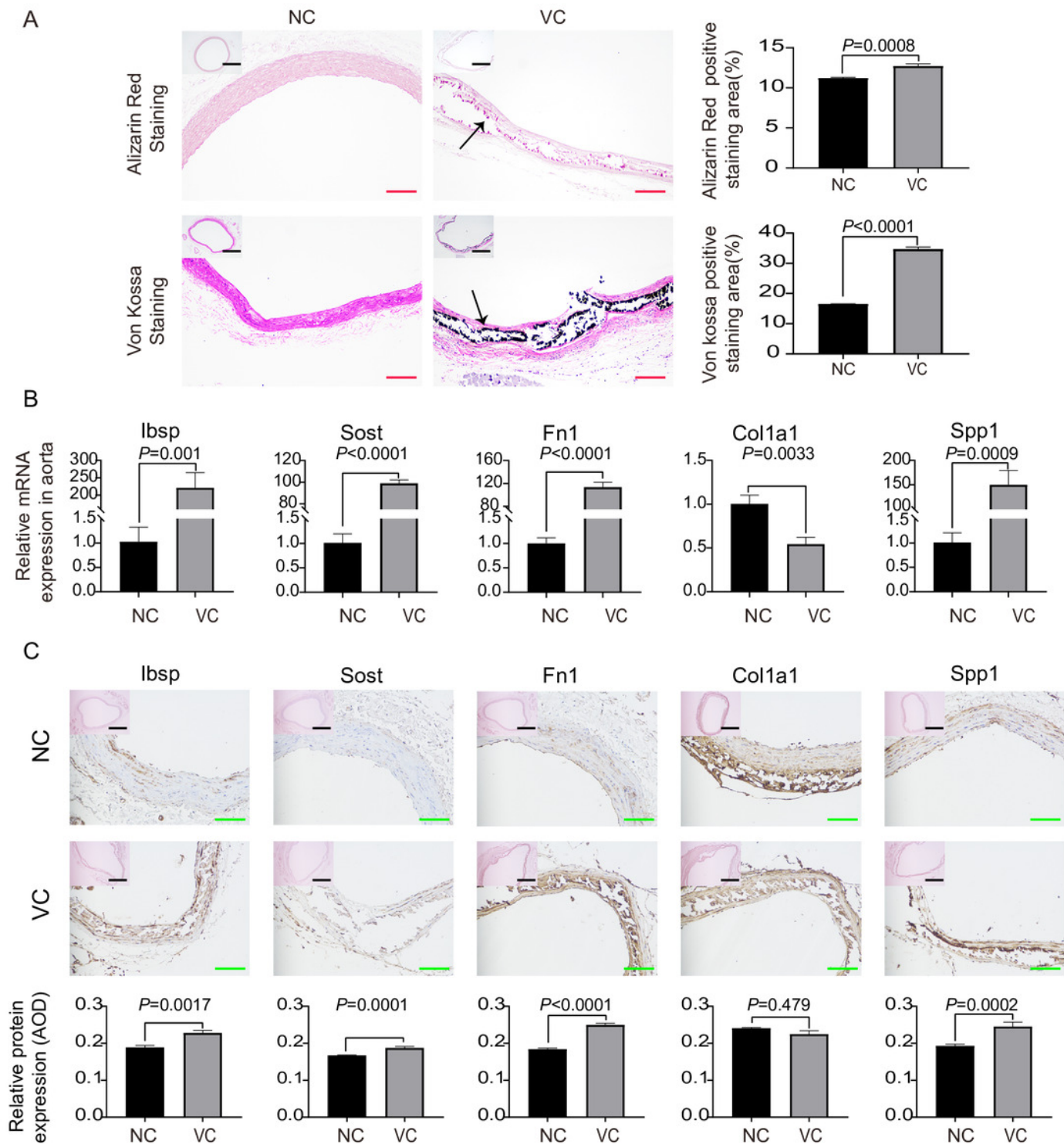
Figure 9

GSEA and Subcellular localization of each hub gene

(A) GSEA of Ibsp. (B) GSEA of Sost. (C) GSEA of Fn1. (D) GSEA of Col1a1. (E) GSEA of Spp1.

(F)Subcellular localization of each hub gene.

Figure 10

miRNA-mRNA network construction and functional enrichment analysis of hub genes.

(A) miRNA-mRNA network construction. (B) Functional enrichment analysis.

Figure 11

TF-mRNA network construction and functional enrichment analysis of hub genes.

(A) TF-mRNA network construction. (B) Functional enrichment analysis.
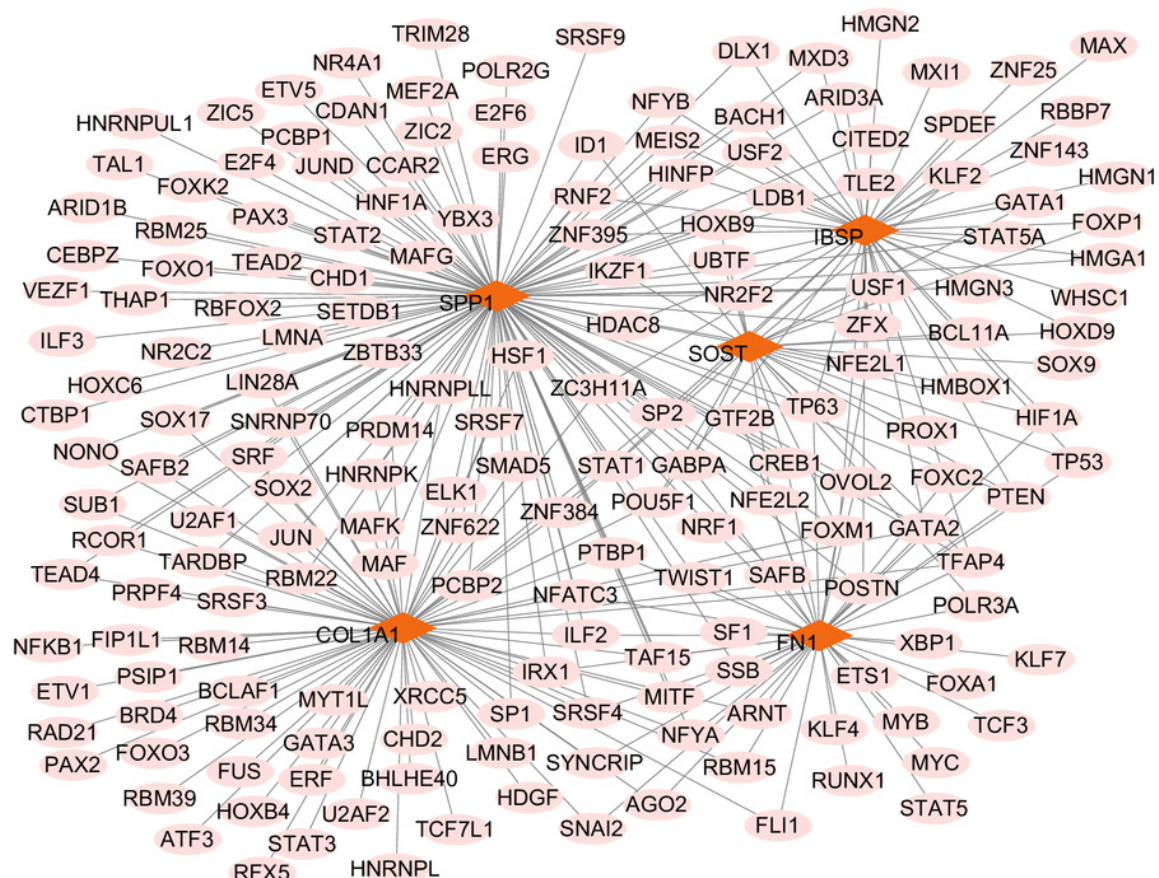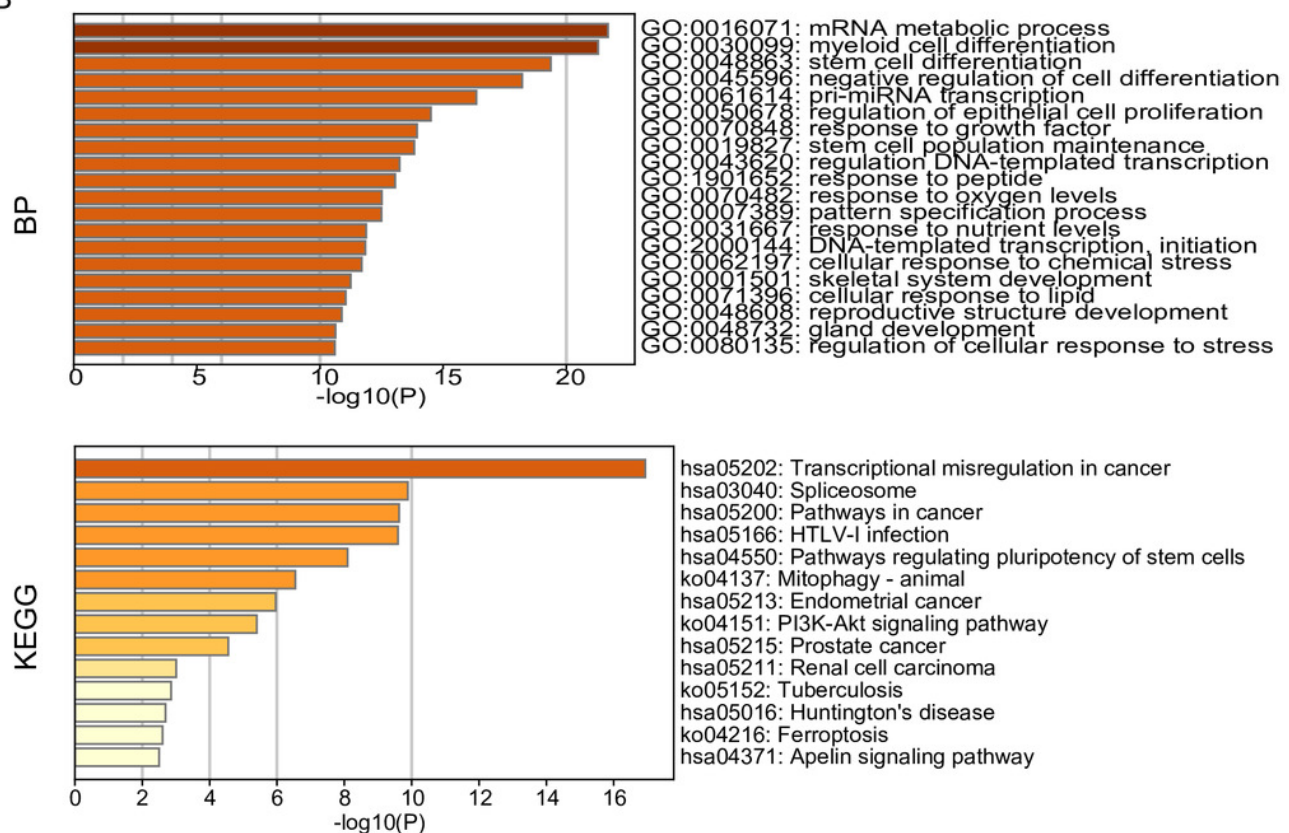
Figure 12

Drug-gene interaction.

The drugs targeting hub genes were obtained by using the DGIdb database. The black line represents inhibited interactions. The gray line represents unknown interactions.
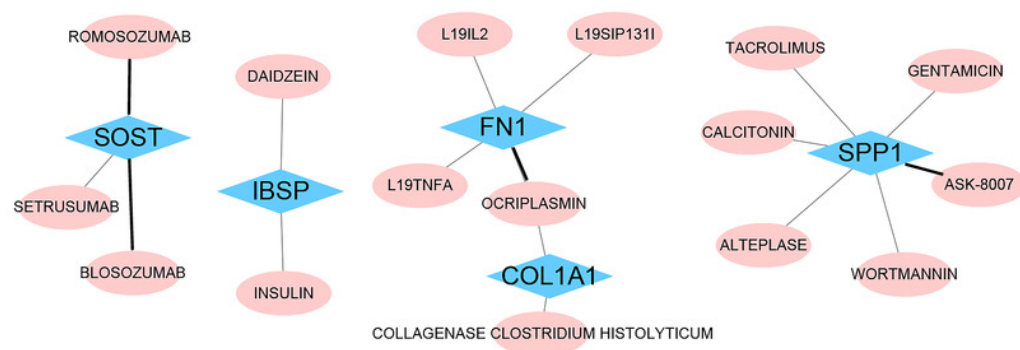
RT-qPCR primers for genes.

1   *Table 1*. RT-qPCR primers for genes

Gene		Primer Sequence
IBSP	Forward	5'-CACTGGAGCCAATGCAGAAGA-3'
	Reverse	5'-TGGTGGGGTTGTAGGTTCAAA-3'
SOST	Forward	5'-CAGCTGTTTTTGTCTGCCCC-3'
	Reverse	5'-GTCATCCACCTGCAGAGCTT-3'
FN1	Forward	5'-CCACAGCCATTCCTGCGCCA-3'
	Reverse	5'-TCACCCGCACTCGGTAGCCA-3'
COL1A1	Forward	5'-GAGGGCCAAGACGAAGACATC-3'
	Reverse	5'-CAGATCACGTCATCGCACAAC-3'
SPP1	Forward	5'-GAAGTTTCGCAGACCTGACAT-3'
	Reverse	5'-GTATGCACCATTCAACTCCTCG-3'
β-Actin	Forward	5'-GGAGATTACTGCCCTGGCTCCTA-3'
	Reverse	5'-GACTCATCGTACTCCTGCTTGCTG-3'